Heliyon 11 (2025) e42074

Contents lists available at ScienceDirect

Heliyon

journal homepage: www.cell.com/heliyon

Research article

Comprehensive metabolite profiling and evaluation of anti-nociceptive and anti-inflammatory potencies of *Nypa fruticans* (Wurmb.) leaves: Experimental and in-silico approaches

Farhana Islam [a,b,c], Md. Aktaruzzaman [b,c], Md. Tarikul Islam [c,d], Fariya Islam Rodru [c,e], Saquiba Yesmine [a,*]

[a] *Department of Pharmacy, Jahangirnagar University, Savar, Dhaka, 1342, Bangladesh*
[b] *Department of Pharmacy, Jashore University of Science and Technology, Jashore, 7408, Bangladesh*
[c] *Laboratory of Advanced Computational Biology, Biological Research on the Brain (BRB), Jashore, 7408, Bangladesh*
[d] *Department of Genetic Engineering and Biotechnology, Faculty of Biological Science and Technology, Jashore University of Science and Technology, Jashore, 7408, Bangladesh*
[e] *Department of Agriculture, Bangladesh Sheikh Mujibur Rahman Agricultural University, Gazipur, 1706, Bangladesh*

ARTICLE INFO

Keywords:
Nypa fruticans
Anti-inflammatory activity
Analgesic
HPLC
COX-2
Molecular dynamic simulations

ABSTRACT

Globally, inflammation and pain are among the most prevalent health issues. The use of medicinal plants to alleviate these conditions is growing. This study comprehensively investigated the analgesic and anti-inflammatory properties of the ethyl-acetate extract of *Nypa fruticans* (EENF) leaves, traditionally used in folk Medicine. High-performance liquid chromatography (HPLC) and gas chromatography-mass spectroscopy (GC-MS) were employed to identify the phytochemicals in EENF. *In vitro* antioxidant studies were conducted to determine the antioxidative properties of EENF. Formalin-induced paw edema assay was employed to assess the *in-vivo* anti-inflammatory activity whereas; acetic acid-induced writhing test, hot plate test, and tail immersion test were performed to evaluate the *in vivo* anti-nociceptive effects. The identified compounds were subsequently evaluated by computational studies against the cyclooxygenase-2 enzyme. EENF demonstrated significant antioxidant activity in both the DPPH scavenging assay (IC_{50}: 105.18 μg/mL) and the reducing power assay (RC_{50}:1752.76 μg/mL). In the *in-vivo* anti-inflammatory assay, EENF exhibited the highest (50.39 % and 67.72 %) inhibition of edema at the fourth hour at 200 and 400 mg/kg body weight, accordingly. Moreover, all the pain modulation studies demonstrated significant ($p < 0.001$) analgesic properties of EENF in a dose-dependent manner. Among, the 23 identified phyto-compounds, the most promising ones were determined to be potential anti-nociceptive and anti-inflammatory agents through molecular docking studies and ADME/T analysis. Molecular dynamics simulations (MDS) confirmed the stability of the protein-ligand complexes. Two phytochemicals, (−) Epicatechin (CID 72276) and Quercetin (CID 5280343), outperformed the standard anti-inflammatory drug, diclofenac sodium, in MDS studies. Both experimental and *in-silico* studies have scientifically verified the traditional use of *Nypa fruticans* in treating pain and inflammatory disease. Overall, (−) Epicatechin and Quercetin possess excellent potential as natural lead compounds for COX-2 inhibition. Further research, including pure compound isolation and biomolecular studies, is needed to understand the underlying mechanisms of these activities.

* Corresponding author. Department of Pharmacy, Jahangirnagar University, Savar, Dhaka, 1342, Bangladesh.
E-mail address: s.yesmine@juniv.edu (S. Yesmine).

https://doi.org/10.1016/j.heliyon.2025.e42074
Received 20 October 2024; Received in revised form 15 January 2025; Accepted 16 January 2025
Available online 21 January 2025

Abbreviation:

EENF	Ethyl acetate Extract of *Nypa fruticans*
PPS	Preliminary phytochemical screening
DPPH	2,2-diphenyl-1-picrylhydrazyl
GC-MS	Gas chromatography-mass spectrometry
HPLC	High-performance liquid chromatography
COX-2	Cyclooxygenase-2
ROS	Reactive Oxygen Spices
OPLS3e	Extending Force Field Coverage for Drug-Like Small Molecules
TIP3P	Transferable intermolecular potential with 3 points
ADME/T	Absorption, Distribution, Metabolism, Excretion and Toxicity
SID	Simulation Interaction Diagram
RMSD	Root means square deviation
RMSF	Root means square fluctuation
Rg	Radius of gyration
SASA	Solvent accessible surface area

1. Introduction

Pro-inflammatory mediators released during an immune response activate immune cells, disrupting homeostasis and contributing to disease development. Nearly all contemporary human illnesses are linked to inflammation [1]. The primary mechanism behind inflammation is the activation of pro-inflammatory mediators including cyclooxygenase-2 (COX-2), cytokines (IL-1β, IL-6, and TNF-α), and inducible nitric oxide synthase (iNOS); that will trigger signaling pathways such as MAPK, NF-κB, PI3K/Akt, and JAK-STAT. Dysfunction in these routes may result in various immunological disorders, like inflammation and cancer. Consequently, these pathways are considered an important target for reducing the symptoms of a variety of inflammatory illnesses [2–4]. Moreover, mild inflammation might be beneficial to promote metabolic processes and aid in the immune system's elimination of harmful substances, such as pathogens, metabolites, necrotic tissue, and inflammatory agents.

On the other hand, uncontrolled or worsening inflammation causes tissue damage, while reactive oxidative stress (ROS), and pain are also present that lowers one's quality of life and productivity at work. It may ultimately lead to a partial loss of bodily functioning. Effective inflammation management strategies may minimize ROS and ease discomfort [5,6]. Additionally, antioxidants mitigate oxidative stress, reduce inflammation, avert cellular damage, and enhance general cellular health by neutralizing ROS [7]. Both steroidal anti-inflammatory drugs (SAIDs) and non-steroidal anti-inflammatory medications (NSAIDs) are currently available on the market for reducing inflammation and the symptoms that are linked to certain inflammatory diseases. Due to their potential adverse effects on several organs, including gastric ulcer, gastrointestinal bleeding, liver dysfunction, heart and kidney failure, allergic reaction, neurologic reaction and other adverse consequences, a worldwide initiative is now being undertaken to identify novel anti-inflammatory medications [8].

Pain is another complicated and diverse issue that may occur from trauma, inflammation, or optic nerve impairment that greatly affects the overall quality of life. The activation of nociceptors (pain receptors) is the mechanism by which pain is experienced. These receptors transmit signals through the spinal cord to the brain, where they are perceived as pain. Substance P and glutamate are among the neurotransmitters and pathways that are involved in this process [9]. It is imperative to create novel analgesics because existing treatments frequently have drawbacks, including insufficient relief for specific types of pain, tolerance, and adverse effects. Innovative analgesics are designed to more effectively target specific pain pathways, resulting in improved pain management with fewer adverse effects. This continual research is essential for the improvement of patient outcomes and the enhancement of overall well-being.

Cyclooxygenase-2 (COX-2) is a crucial protein in the inflammatory process, responsible for the synthesis of prostaglandins, that are lipid compounds involved in pain, fever, and inflammation [10]. Unlike COX-1, which is occurs naturally across all tissues, COX-2 is produced during inflammation in response to stimuli like cytokines, growth factors, and endotoxins, making it a more specific target for analgesic drugs [11]. Targeting COX-2 can effectively lower inflammation, and pain with decrease gastrointestinal side effects in contrast to non-selective COX inhibitors. This specificity makes COX-2 an attractive target for developing novel analgesics that provide better pain relief while minimizing adverse effects. The physiological function of plant medicines including antioxidant, analgesic, anti-inflammatory, and antipyretic characteristics is inherently linked to the existence of their metabolites [12]. Furthermore, compounds including terpenes, flavonoids, and alkaloids can directly influence metabolic cascades and receptors to modify analgesic and inflammatory responses [13].

Mangrove plants are very effective at scavenging free radicals because of their harsh environment including low oxygen, high salinity, strong wind, and water logging [14]. They are rich in a variety of metabolites, such as vitamins, terpenoids (like carotenoids), phenolic compounds (like phenolic acids, quinones, flavonoids, coumarins, tannins, and lignans), nitrogen compounds (like amines, alkaloids, and betalains), and several other natural compounds with hypoglycemic and antioxidant qualities [15]. *Nypa fruticans* Wurmb. (Aceraceae), commonly known as 'Gol Pata' in Bangladesh, is one of the most significant trees that make up the botanical wealth of the mangroves [16]. The Nypa palm is regarded as an "underutilized" plant and is located in the Philippines, Malaysia,

Indonesia, India, and certain regions of Queensland, Australia [17]. In modern medicine, plenty of phytochemicals of nipa used as raw materials. Different parts of *N. fruticans* such as; fruits, sap (nipa palm vinegar), stem, shoots and roots are conventionally utilized to cure asthma, diabetes, leprosy, tuberculosis, liver disease, kidney stone, sore throat, snake bite, pain, inflammation and are also used as sedative and carminative [17–19] In contrast, the leaves of *Nypa fruticans* remain largely unexplored, despite their potential. Previous scientific research revealed various pharmacological activities of different parts of *N. fruticans* including antioxidant, anti-inflammatory, anticancer, antinociceptive, and anti-diabetic but comprehensive analysis of analgesic and anti-inflammatory properties of *N. fruticans* leaves is yet to be investigated [2,17]. Therefore, the goal of our current research was to systematically explore the antioxidant, anti-nociceptive, and anti-inflammatory activities of *N. fruticans* leaves through experimental and *in-silico* approaches to reveal potential target insights of the bioactive compounds followed by determining the potential lead compounds.

2. Material and methods

2.1. Chemicals and reagents

Sigma-Aldrich (St. Louis, Missouri, USA) supplied the following compounds: ascorbic acid, aluminum chloride, sodium carbonate, quercetin, DPPH (2, 2-diphenyl-1-picrylhydrazyl), gallic acid, acetic acid, Folin-Ciocalteau reagent (FCR), methanol, and sodium hydroxide. Besides, Merck (Darmstadt, Germany) provided the butylated hydroxytoluene (BHT), ferric chloride, potassium ferricyanide, phosphate buffer, sodium nitrite, and trichloro-acetic acid (TCA). Beximco Pharmaceuticals Ltd. in Bangladesh supplied the three standard drugs (indomethacin, diclofenac and tramadol). All reagents were of analytical grade.

2.2. Collecting plant materials and preparing crude extract

In January 2022, the fresh leaves of *N. fruticans* were gathered from healthy host plants of Sundarbans, the biggest mangrove forest in the world, in Khulna, Bangladesh. The collected plant sample was identified and certified by Khandakar Kamrul Islam, Senior Scientific Officer, Bangladesh National Herbarium, Ministry of Environment, Forest and Climate Change, Bangladesh. For subsequent use, a sample voucher (DACB: 92809) has been preserved at the Herbarium.

After being cleaned, the gathered leaves were allowed to dry for three weeks in the shade; ground into a fine powder utilizing a laboratory grinding mill (Model 2000 LAB Eriez®), and sieved through a 40-mesh screen. For extraction, 300 g of powdered *N. fruticans* were immersed in 1700 mL of ethyl acetate, allowing it to macerate for fourteen days with periodic shaking and agitation. Then Whatman Grade 1 filter paper (Sigma-Aldrich, St. Louis, MO, USA) was used to filtrate the mixture. With the help of a rotating vacuum evaporator (Buchi Rotavapor Model R-124) the filtrate was evaporated at 36 °C and 40 rpm and dried in desiccators. This process produced 5.8 g of extract, yielding a 1.93 % (w/w), and preserved in an airtight container at 4 °C to prevent microbial growth.

2.3. Phytochemical screening

Several qualitative tests on freshly prepared EENF extract were conducted to reveal the presence of different secondary metabolites [20,21].

2.4. Determination of total phenolic content

The total phenolic content (TPC) of EENF was evaluated utilizing the Folin-ciocalteu (FC) reagent, as demonstrated by Sarkar et al., 2022 [20,22] by employing a standard curve of gallic acid at numerous concentrations ranging from 100 μg/mL to 500 μg/mL. Initially, 9 mL of distilled water and 1 mL of FC reagent (10 % v/v) were added to 1 mL of the solution from each concentration in separate volumetric flasks. After 5 min, distilled water was added with 10 mL of a 7 % w/v sodium carbonate solution to adjust the volume to 25 mL. The absorbance was measured at 750 nm after 30 min of incubation using a blank solution as the reference. The TPC was calculated in milligrams of gallic acid equivalent per gram of extract (mg GAE/g).

2.5. Total flavonoid content assay

The total flavonoid content (TFC) of EENF was evaluated employing a standard quercetin calibration curve [20,23]. One mL of quercetin solution from each concentration was added with 4 mL of distilled water, in a volumetric flask, followed by 0.3 mL of sodium nitrous solution (5 % w/v). Once the mixture had been incubated for 5 min, 0.3 mL of aluminum chloride (10 % w/v) was added to it. Then, a final volume of 10 mL was adjusted after adding 2 mL sodium hydroxide (1 M). In the next step, the absorbance was measured at 510 nm against a blank solution and the results were expressed as mg quercetin equivalent (QE) per g of extract (mg QE/g).

2.6. Determination of total tannin content

The total tannin content (TTC) of EENF was determined utilizing Folin-Ciocalteu's method [15]. To determine the TTC, 10 mg of extract was diluted with 10 mL of distilled water to prepare a concentration of 1 mg/mL. Gallic acid was used at various concentrations to generate the standard calibration curve. Folin-Ciocalteu's reagent (0.5 mL) and extract solution (0.1 mL) were mixed with 7.5 mL of distilled water, followed by the addition of 1 mL of 35 % (w/v) Na_2CO_3 solution to bring the final volume to 10 mL. After 30 min of

incubation, the absorbance was measured at 725 nm against a blank using a UV spectrophotometer. The amount of TTC in EENF was expressed as milligrams of gallic acid equivalent per gram of plant extract (mg GAE/g).

2.7. Profiling of polyphenol compounds through HPLC

A portion of the polyphenolic components of EENF was determined and measured employing HPLC-DAD analysis [24,25]. A Shimadzu (LC-20 A, Japan) with a column oven (CTO-20 A), auto sampler (SIL-20A HT), photodiode array detector (SPD-20A), and binary solvent delivery pump was utilized by the HPLC examination. The separation was done at 33 °C using a Luna C18 (5 μm) Phenomenex column (4.6 × 250 mm). With gradient elution, the study employed a mobile phase made up of A (1 % acetic acid in acetonitrile) and B (1 % acetic acid in water): 0.01–20 min (5–25 % A), 20–30 min (25–40 % A), 30–35 min (40–60 % A), 35–40 min (60–30 % A), 40–45 min (30–5% A), and 45–50 min (5 % A). After setting the flow rate to 0.5 mL/min, 20 μL of the sample was injected. To validate the methodology and evaluation, the ultraviolet sensor was turned on at a wavelength of 270 nm. A 0.45 μm Nylon 6, 6 membrane filter (India) was used to filter the mobile phase, and it was vacuum-degassed thereafter. A typical stock solution was developed in methanol in order to produce a calibration curve with the following contents: 20 μg/mL of Gallic acid; 15 μg/mL of 3, 4-Dihydroxybenzoic acid; 50 μg/mL of Catechin hydrate; 30 μg/mL of Catechol, (−) Epicatechin, and Rosmarinic acid; 10 μg/mL of Caffeic acid, Vanillic acid, Syringic acid, Rutin hydrate, p-Coumaric acid, trans-Ferulic acid, and Quercetin; 8 μg/mL of Myricetin, Kaempferol; and 4 μg/mL of trans-Cinnamic acid. Additionally, the limits of detection for (−)-Epicatechin, Caffeic acid, Rutin hydrate, Rosmarinic acid, Myricetin, Quercetin, Trans-Cinnamic acid, and Kaempferol were 0.15, 0.07, 0.07, 0.16, 0.10, 0.04, 0.05, and 0.11 ppm, respectively whereas; the resolutions for these compounds were 2.018, 2.399, 16.688, 27.223, 3.640, 18.386, 7.350, and 3.594, respectively.

2.8. GC-MS analysis

The GC-MS study was performed by employing a Clarus® 690 gas chromatograph furnished with a column Elite-35 (30 m × 0.25 mm, 0.25 m film) and a Clarus® SQ 8 C mass spectrometer. Following spitless mode, 1 μL of the sample was injected into the chamber, and 99.999 % pure helium was adopted as the gas transporter, flowing consistently at 1 mL/min throughout the 40-min trial. In this analysis, the resolution was 1.000 amu (Mass) (Scans; 1) and the limit of detection was set at 0.02 mg/mL. Initially, the column temperature of the oven was fixed at 60 °C (for 0 min) and then by a continuous rise of 5 °C each minute till it reached 240 °C, and was maintained for 4 min. The National Institute of Standards and Technology (NIST) conducted a database search to ascertain the contents of the samples [26].

2.9. In vitro investigation of antioxidant activity

2.9.1. DPPH free radical scavenging assay

A technique described earlier was followed in the DPPH free radical scavenging study to determine the antioxidant potential of EENF [27]. Several concentrations (1024–2 μg/mL) of both the standard and the extract were made utilizing the serial dilution method. later, 6 mL of alcoholic DPPH solution (0.004 % w/v) was combined with 2 mL of standard and extract solutions from each concentration. Applying a UV–visible spectrophotometer (made in Shimadzu, Japan) the absorbance was measured at 517 nm after 30 min of incubation (in a dark place). Ascorbic acid was utilized as the standard antioxidant for comparison. The DPPH scavenging potential was estimated using the following formula:

$$\textbf{Scavenging}\ (\%) = \left[\mathbf{1}\ \left(\mathbf{ASample}\ /\ \mathbf{Standard}\ /\ \mathbf{A_{Control}}\right)\right] \times \mathbf{100}.$$

The IC_{50} value was measured by comparing the data of ascorbic acid.

2.9.2. Reducing power assay

The reducing power assay was executed according to the guidelines provided in Kishore et el [20]. Various concentrations of EENF and standards were made, ranging from 100 to 500 μg/mL.

Then, 2.5 mL of phosphate buffer (200 mmol/L, pH 6.6) and 2.5 mL of potassium ferricyanide (1 % w/v) were mixed with 1 mL of an aliquot from each concentration. The mixture was incubated for 20 min, after which it was combined with 2.5 mL of 10 % (w/v) trichloroacetic acid. Subsequently, 2.5 mL of the supernatant was collected after centrifugation at 3000 rpm for 10 min and blended with 0.5 mL of ferric chloride (0.1 % w/v), with continuous shaking. Finally, after 5 min, the absorbance was recorded at 700 nm in contrast to a blank solution.

2.10. Experimental animals

Swiss albino mice (male, aged 6–7 weeks) weighing between 25 and 28 g, were used in this study. The mice were maintained in an environment with 12 h of light and dark cycles, a relative humidity of 55–65 %, and a temperature of (27.0 ± 1.0) °C at the animal studies laboratory, department of Pharmacy, Jahangirnagar University, Bangladesh. Ad libitum consumption of distilled water and nutritious food was given to the test animals. All experimental studies in this research were conducted following the guidelines of the Organization for Economic Cooperation and Development (OECD) [28]. Additionally, the Biosafety, Biosecurity, and Ethical

Committee of Jahangirnagar University issued instructions, which were also followed for all *in vivo* investigations [Ref No: BBEC, JU/M 2023/11 (68)].

2.11. Study of acute toxicity

An acute toxicity study was executed in accordance with the requirements provided by the OECD [28]. Thirty-five overnight (16 h) fasted mice (25–30 gm) of both sexes were divided into seven groups (n = 5). EENF was given orally to each group at 200, 400, 1000, 2000, 3000, and 4000 mg/kg; body weight and the vehicle was supplied distilled water. All groups were carefully monitored for fourteen days to detect any toxicological effects, including changes in skin, lethargy, coma, diarrhea, and salivation, to determine any signs of toxicity [29].

2.12. In vivo analgesic activity study

2.12.1. Acetic acid-induced writhing test

Published protocol was followed to conduct the acetic acid-induced writhing assay with minor modifications [20]. The mice were separated into four groups following randomization manner, with five mice in each. After overnight fasting, the control received distilled water (10 mL/kg; b.w), the standard group got Diclofenac sodium (25 mg/kg; b.w) and the treatment groups were administered with EENF at 200 and 400 mg/kg; body weight accordingly. Subsequently, 30 min before to the oral administration of the experimental samples, an intraperitoneal injection of 0.7 % (v/v) acetic acid solution was injected to induce pain. Accompanying a 5-min break, the number of writhes was counted for 10 min and the percentage of writhing suppression was calculated by applying a particular equation:

$$\% \text{ Inhibition of writhing} = (1 - w_0 / w_1) \times 100$$

The variables " w_1" and " w_0" depicted the mean quantity of writhing in the control and standard or sample groups, accordingly.

2.12.2. Tail immersion test

The pain responses were measured by tail immersion method among the groups discussed above, where tramadol (10 mg/kg) was given as a standard [20]. A 15-s threshold time was considered, and the latency period of tail-flick responses was recorded after 0, 30, 60, 120, and 180 min of corresponding therapy.

2.12.3. Hot plate method

A hot plate study [30] was conducted with the control (distilled water; 10 mL/kg; bw), standard (tramadol; 10 mg/kg, bw), and treatment groups (EENF; 200 mg/kg and 400 mg/kg, bw). Each medication was delivered orally 30 min before recording latency responses. A variety of factors, including licking, leaping, and dropping the paw from the hot plate, were observed to assess the latency response at 0, 30, 60, 120, and 180-min intervals.

2.13. In vivo anti-inflammatory activity by formalin induced inflammation model

Formalin-induced paw edema assay was applied to assess the *in vivo* anti-inflammatory activity. For measuring the formalin-induced inflammation [31], twenty mice were split into four groups (n = 5/group): control, disease control, and treatment groups; the control received distilled water (10 mL/kg), the standard given indomethacin (10 mg/kg b.w.), and the treatment groups given EENF at doses of 200 and 400 mg/kg body weight accordingly. The doses were received orally 30 min prior to formalin administration, and the paw circumference was calculated at 1, 2, 3, 4, 24, and 48 h by a plethysmometer (LE 7500-plan lab S.LU, Spain). The percentage of inhibition of edema was enumerated as:

$$\% \text{ Inhibition} = [(1 - l_1) / l_0) \times 100]$$

where; l_0 = The control paw's average circumference, and l_1 = The standard or sample paw's average circumference.

2.14. Statistical analysis

All results were revealed as the mean ± SEM (standard error of the mean). A one-way ANOVA was used to analyze several comparisons, and then a post-hoc Dunnett's test was conducted. We considered the effects significant when $^*p < 0.05$, $^{**}p < 0.01$, or $^{***}p < 0.001$. SPSS (version 9) was applied to perform statistical analysis.

2.15. In-silico studies

2.15.1. Ligand preparation

GC-MS and HPLC analysis of *N. fruticans* leaf extract revealed 23 compounds that were considered for molecular docking study. The structures of isolated metabolites and the control compound (Diclofenac) were obtained in SDF format from the PubChem database (http://www.pubchem.ncbi.nlm.nih.gov/). The LigPrep module of Maestro Schrodinger Suite v11.4 was utilized to process, prepare,

and refine the ligands [32].

2.15.2. Protein preparation

The 3D structure of COX-2 (PDB ID: 5KIR) was retrieved from the PDB (Protein Data Bank) database (http://www.rcsb.org/). In the COX-2 protein, the amino acid sequence chains for A, and B, are 551 with a resolution of 2.70 Å [33]. The protein preparation wizard of the Schrodinger suite 2020–3 was used to remove unnecessary chains, metals, water, and co-factors [34]. Using the OPLS-3e force field, the 3D crystal structure of the protein was optimized [35].

2.15.3. Receptor grid generation and molecular docking study

The *in-silico* study was carried out to determine the most suitable drug candidates for the target receptor [36–38]. In this step, previously prepared compounds were docked with the selected protein using the Glide v-8.8 and Maestro v-12.5.139 packages from the Schrodinger Suite [32]. The OPLS3e force field in standard precision (SP) mode was used in overall molecular docking [39]. The native inhibitor (N3) in combination with protein was used to grids generate the receptor [40]. The ascertained chemicals along with the control drugs were utilized for molecular docking with the target receptor (5KIR). The grid box was positioned at X = 23.23, Y = 1.36, and Z = 34.42 for 5KIR. The molecular interactions of ligands with the target protein were determined by calculating binding affinities. The Maestro viewer was used to observe the different chemicals and ligand-binding residues.

2.15.4. ADME and toxicity analysis

Absorption, distribution, metabolism, excretion, and toxicity (ADME/T) are one of the sets of biological parameters focused on drug development and discovery [36]. It is crucial to understand how a drug candidate is processed by a living organism in the early stages of drug design and development [41]. The Swiss ADME (http://www.swissadme.ch) server was employed to assess the pharmacodynamic response of the selected phytochemicals [42]. As part of the drug development process, toxicology testing is important in determining the molecule's toxic properties and dose requirements. Therefore, the ProTox-II server (http://tox.charite.de/protox_II) was used to evaluate the initial-stage toxicity of the selected phytochemicals, including cytotoxicity, hepatotoxicity, mutagenicity, carcinogenicity, and immunotoxicity [43].

2.15.5. Molecular dynamic simulation of protein-ligand complexes

MD simulation is a tool for analyzing the physical properties and behavior of molecules in an artificial macromolecular environment. In this study, we utilized the Desmond module of Schrödinger (Academic version) for the MD simulation, and all the analyses were performed under a Linux environment (Release 2022–4) [44,45]. The predefined simple point-charge (SPC) water model was used to simplify the complex system so that water density and permittivity can be accurately determined. To ensure an appropriate volume on both sides, a TIP3P water model preset with its orthorhombic periodic boundary box shape of $10 \times 10 \times 10$ Å^3 was used. To maintain electrical neutrality, ions such as Na^+ and Cl^- were added, achieving a 0.15 M salt concentration throughout the entire system. A constant pressure of 0.10925 bar and a temperature of 300 K were used in the isothermal-isobaric (NPT) ensemble. The OPLS3e force field was applied to optimize the system [39].

2.15.6. MD trajectory analysis

Schrödinger Maestro interface v9.5 was employed to render simulation snapshots at 2 PS intervals for each atomic movement. The simulation events were observed applying the simulation interaction diagram (SID). Various simulation features including, root-mean-square fluctuations (RMSF), root-mean-square deviations (RMSD), the radius of gyration (Rg), and solvent-accessible surface area (SASA), were also considered from the trajectory output.

Table 1
Phytochemical screening of EENF.

SN	Classes of phytochemicals	EENF
1.	Alkaloids	+
2.	Tannins	+
3.	Glycoside	+
4.	Steroids	+
5.	Carbohydrates	+
6.	Coumarins	–
7.	Saponins	+
8.	Phenolic compounds	+
9.	Flavonoids	+
10.	Triterpenes	+
11.	Gum	+

Here, "+" represent the presence, and "-" represent the absence.

3. Results

3.1. Qualitative analysis of phytochemicals

Table 1 reports the detection of therapeutically active secondary metabolites in EENF following phytochemical screening. Significant phytochemicals like alkaloids, carbohydrates, tannins, glycosides, steroids, saponins, phenolic, and flavonoid compounds, triterpenes, and gum were present in EENF.

3.2. Acute toxicity study

Evaluation of acute toxicity of EENF at different doses (200, 400, 1000, 2000, 3000, and 4000 mg/kg; b.w.) exhibited in no visible signs of acute toxicity, and no fatalities during the course over the fourteen days. These results indicated that the extract's LD50 (lethal dose in 50 %) was higher than 4000 mg/kg body weight.

3.3. Chemical profiling through HPLC analysis

We conducted an HPLC analysis to determine the quantity of polyphenols in EENF. Figs. 1 and 2 depict the chromatographic separations and polyphenol determination in the standard and EENF, respectively. Table 2 represent the identified eight phenolic compounds of EENF with their quantity and pharmacological significance. EENF had the highest content of (−) epicatechin (36.32 ± 0.15 mg/100 g dry extract) among measured polyphenols, but only a moderate amount of trans-cinnamic acid (8.94 ± 0.10 mg/100 g dry extract), rutin hydrate (7.48 ± 0.11 mg/100 g dry extract), and quercetin (4.76 ± 0.08 mg/100 g dry extract). Smaller amounts of caffeic acid, kaempferol, myricetin, and rosmarinic acid were also found: 1.64 ± 0.02, 1.28 ± 0.04, 1.24 ± 0.05 and 0.27 ± 0.02mg/100 g of dry extract, in that order.

3.4. Identification of phytochemicals by GC-MS

GC-MS analysis revealed 15 phytochemicals from the extract, arranged in Table 3 by their retention time (RT), molecular formula, peak area (%), phytochemical name, molecular weight, molecular formula and their pharmacological significance. According to the GC-MS chromatogram (Fig. 3), the ascertained four major compounds were hexadecanoic acid, 1-(hydroxymethyl)-1,2-ethanediyl ester (25.70 %), N-hexadecanoic acid (11.91 %), L-(+)-ascorbic acid 2,6-dihexadecanoate (4.97 %), and cyclotrisiloxane 2,4,6-trimethyl-2,4,6-triphenyl- (4.08 %).

3.5. Total phenolic content (TPC)

We calculated the TPC using a gallic acid calibration curve (y = 0.0035× - 0.0273; R2 = 0.985). In EENF, the maximum amount of TPC was discovered to be 239.87 ± 1.36 mg GAE/g dry extract.

3.6. Total flavonoid content (TFC)

With the help of the standard quercetin calibration curve (y = 0.001× - 0.0067, R2 = 0.984), it was found that EENF had the highest level of TFC and that is 225 ± 1.13 mg QE/g dry extract.

3.7. Total tannin content (TTC)

EENF exhibited significant amount of TTC (103.70 ± 0.72 mg GAE/g dry extract), which was measured from the gallic acid calibration curve (Y = 0.0143X + 0.1375; R2 = 0.9865).

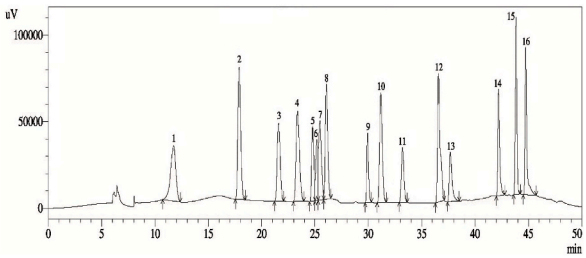

Fig. 1. HPLC fingerprint standard mixture of polyphenolic compounds (Peak 1: gallic acid; Peak 2: 3,4-dihyrdoxybenzoic acid; Peak 3: catechin hydrate; Peak 4: catechol; Peak 5: (−) epicatechin; Peak 6: caffeic acid; Peak 7: vanillic acid; Peak 8: syringic acid; Peak 9: rutin hydrate; Peak 10: p-Coumaric acid; Peak 11: Trans-Ferulic acid; Peak 12: Rosmarinic acid; Peak 13: Myricetin; Peak 14: Quercetin; Peak 15: Trans-Cinnamic Acid; Peak 16: Kaempferol.).

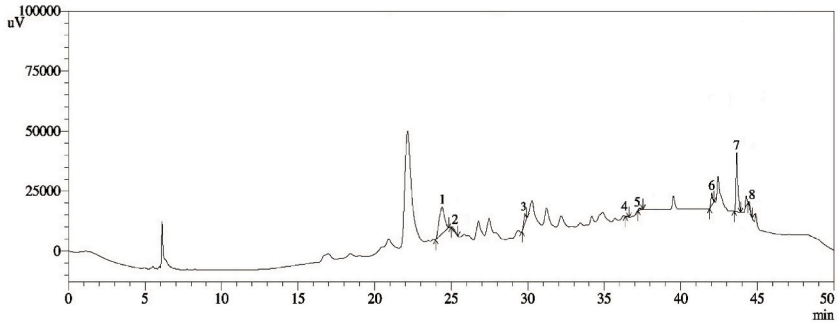

Fig. 2. The HPLC fingerprint of *N. fruticans* (1. (−) Epicatechin, 2. Caffeic acid, 3. Rutin hydrate, 4. Rosmarinic acid, 5. Myricetin, 6. Quercetin, 7. Trans-Cinnamic acid, and 8. Kaempferol.).

Table 2
Phytochemicals identified from EENF through HPLC.

Standard compounds	EENF (mg/100 g dry extract)	Pharmacological significance	Citation
Gallic acid	ND		
3,4-Dihydroxybenzoic acid	ND		
Catechin hydrate	ND		
Catechol	ND		
(−) Epicatechin	36.32 ± 0.15	Antioxidant, anti-inflammatory, anti-diabetic, neuroprotective, and cardioprotective activity.	[46]
Caffeic acid	1.64 ± 0.02	antioxidant, anti-inflammatory, neuroprotective, anti-diabetic and anticancer activity.	[47]
Vanillic acid	ND		
Syringic acid	ND		
Rutin hydrate	7.48 ± 0.11	Antioxidant, anti-inflammatory, cytoprotective, Vaso protective, anticancer, neuroprotective, cardioprotective activity.	[48]
p-Coumaric acid	ND		
trans-Ferulic acid	ND		
Rosmarinic acid	0.27 ± 0.02	Antioxidant, anti-inflammatory, anticancer, antidiabetic, neuroprotective, antimicrobial, and activity.	[49,50]
Myricetin	1.24 ± 0.05	Antioxidant, anti-inflammatory, anticancer, antimicrobial, cardioprotective, neuroprotective, and anti-diabetic activity.	[51,52]
Quercetin	4.76 ± 0.08	Antibacterial agent, antioxidant, anti-inflammatory, anticancer, cardioprotective, hypercholesterolemia, rheumatic diseases.	[53]
trans-Cinnamic acid	8.94 ± 0.10	Antioxidant, antimicrobial, anticancer, neuroprotective, anti-inflammatory and antidiabetic activity.	[54,55]
Kaempferol	1.28 ± 0.04	Antioxidant, anti-inflammatory, antimicrobial, cardioprotective, anticancer activity.	[56]

3.8. In vitro antioxidant assay

3.8.1. Free radical scavenging action of DPPH

As a crude extract, EENF may not scavenge free radicals as efficiently as standard antioxidants like ascorbic acid, due to its composition of multiple bio compounds. However, its antioxidant activity was exhibited by its IC_{50} value. The IC_{50} value for EENF was 105.18 μg/mL, whereas ascorbic acid exhibited an IC_{50} value of 14.24 μg/mL, as illustrated in Fig. 4.

3.8.2. Assay of reducing power

In the reducing power assay, BHT and EENF showed RC50 values of 1873.41 μg/mL and 1752.76 μg/mL, respectively (Fig. 5). These values were very similar, indicating that EENF demonstrated good antioxidant activity.

3.9. Study of In vivo analgesic activity

3.9.1. Acetic acid-induced writhing test

In this test, EENF at doses of 200 and 400 mg/kg body weight significantly reduced writhing in contrast to the control group ($^*P < 0.001$). Remarkably, the 400 mg/kg dose of EENF produced an 80.07 ± 1.00 % reduction in writhing, which was the most substantial reduction observed in every examined group and was identical to the typical treatment's reduction of 82.3 ± 1.39 %, as illustrated in Fig. 6.

Table 3
Phytochemical composition of EENF identified through GC-MS analysis.

SN	RT	% Area	Name of the compounds with MF	MW (g/mol)	Pharmacological significance	Citation
1	17.77	0.010547	Guaiol ($C_{15}H_{26}O_s$)	222	Antitumor, antibacterial, anti-inflammatory, antimicrobial, antiviral activity	[57]
2	18.55	0.377061	(−)-Aristolene ($C_{15}H_{24}$)	204	Antimicrobial, anti-inflammatory, and anticancer activity	[58,59]
3	19.75	0.64284	2,3-dehydro-4-oxo-.beta.-ionone ($C_{13}H_{16}O_2$)	204	Antimicrobial, antioxidant, anti-inflammatory activity	[60]
4	22.08	3.029866	Neophytadiene ($C_{20}H_{38}$)	278	Anti-oxidant, anti-inflammatory, antimicrobial, anxiolytic, sedative, antidepressant, anti-diabetic activity	[61,62]
5	25.22	2.124966	Phytyl tetradecanoate ($C_{34}H_{66}O_2$)	506	Anti-oxidant, anti-inflammatory, and antimicrobial, anti-diabetic activity	[62]
6	25.60	0.563756	1,5-diphenyl-2h-1,2,4-triazoline-3-thione ($C_{14}H_{11}N_3S$)	253	Antioxidant, anti-inflammatory, analgesic, neuroprotective, antimicrobial, anticancer, anti-urease activity	[63,64]
7	25.85	2.016225	13-docosen-1-ol, (z)- ($C_{22}H_{44}O$)	324	Not found.	
8	26.20	2.453694	Eicosen-1-ol, cis-9- ($C_{20}H_{40}O$)	296	Not found.	
9	29.12	11.91749	N-hexadecanoic acid ($C_{16}H_{32}O_2$)	256	Antioxidant, antimicrobial, anti-inflammatory, hypocholesterolemia and anti-cancer activity	[65,66]
10	31.57	2.503253	Phytyl palmitate ($C_{36}H_{70}O_2$)	534	Antioxidant, anti-inflammatory, cardioprotective and anti-diabetic activity	[67]
11	32.79	4.975571	L-(+)-ascorbic acid 2,6-dihexadecanoate ($C_{38}H_{68}O_8$)	652	Antioxidant, anti-inflammatory, antimicrobial, antimalarial, antiallergic, neuroprotective, antibronchitic, anticancer, hepatoprotective and others activity.	[67]
12	34.55	0.285726	Bis [di (trimethylsiloxy)phenylsiloxy] trimethylsiloxyphenyl siloxane ($C_{33}H_{60}O_7S_8$)	792	Not found.	
13	34.95	1.387688	Z,z-6,27-hexatriactontadien-2-one ($C_{36}H_{68}O$)	516	Antioxidant, antimicrobial, anti-inflammatory and vasodilator activity	[68]
14	35.67	25.70054	Hexadecanoic acid, 1-(hydroxymethyl)-1,2-ethanediyl ester ($C_{35}H_{68}O_5$)	568	Anti- inflammatory, neuroprotection, anti-microbial and anti-cancer activity	[69]
15	37.16	4.082648	Cyclotrisiloxane, 2,4,6-trimethyl-2,4,6-triphenyl- ($C_{21}H_{24}O_3Si_3$)	408	Not found.	

Here; RT = Retention time, MW = Molecular Weight, MF = Molecular formula.

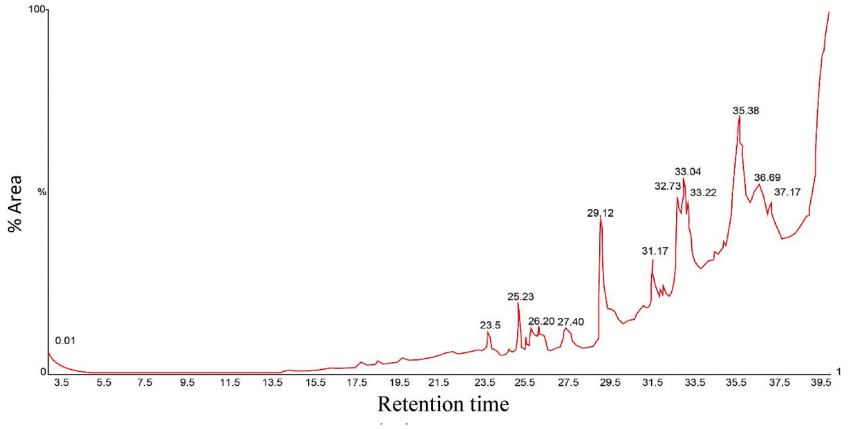

Fig. 3. GC-MS chromatogram of ethyl acetate extract of *N. fruticans*.

3.9.2. Tail immersion test

A notable, time-dependent increase in latency was observed following the administration of higher doses of the EENF extract, with only minor fluctuations (*P < 0.05 compared to the control). The of 400 mg/kg body weight of EENF produced the greatest latency response at the 3rd (60 min) observation period, as shown in Fig. 7.

3.9.3. Hot plate test

A pronounced latency response was observed in a time-dependent manner with tramadol and the extract (EENF 200 and 400 mg/kg, body weight). Compared to the control, the latency response to tramadol and the 400 mg/kg dose of EENF increased progressively from the second to the fifth observation period, reaching a peak at 180 min, as shown in Fig. 8.

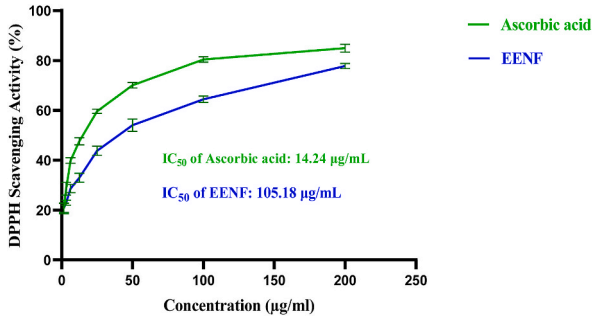

Fig. 4. DPPH radical scavenging properties of EENF in comparison with ascorbic acid.

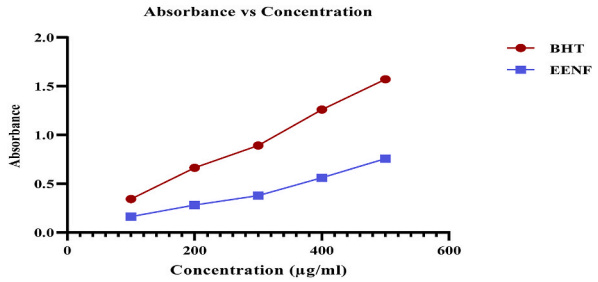

Fig. 5. Illustration of reducing activity of EENF compared to the reference standard (BHT).

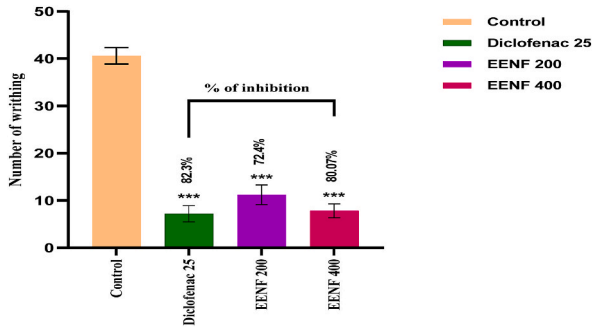

Fig. 6. The impacts of EENF in acetic acid-induced writhing study in mice (n = 5). The findings were stated as mean ± SEM. Comparisons with the control group showed ***p < 0.001, **p < 0.01, and *p < 0.05 to be statistically significant.

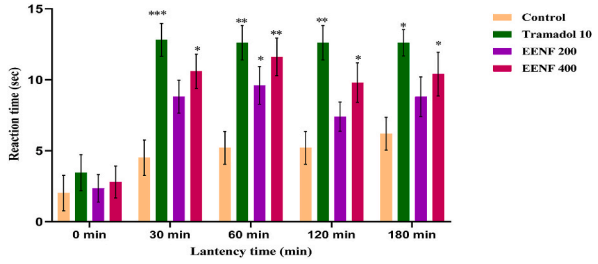

Fig. 7. Effects of EENF in *in vivo* the tail immersion study (n = 5) were reported as mean ± SEM. Statistical comparisons with the control group revealed significance levels of ***p < 0.001, **p < 0.01, and *p < 0.05.

3.10. In vivo anti-inflammatory activity study

After administering EENF at both doses, a significant reduction in paw volume was observed. Fig. 9 shows the percentage inhibition of edema at 200 and 400 mg/kg body weight of EENF compared to the control. However, at the 4th hour following formalin administration, the maximum (400 mg/kg b.w) dose of EENF exhibited the highest inhibitory effect (67.72 %), whereas indomethacin

exhibited the highest response (68.21 %) at the 3rd hour.

3.11. In silico studies

3.11.1. Molecular docking

According to the outcomes of the HPLC and GC-MS analysis, a total of 23 compounds were docked against the COX-2 receptor as part of the molecular docking study. Among them, 9 compounds, CID 72276, CID 5280343, CID 5280863, CID 5281672, CID 5281792, CID 2802516, CID 5363867, CID 444539, and CID 689043 exhibited significantly promising binding affinities with COX-2, showing values of −8.62, and −8.59, −7.69, −5.82, −5.74, −5.49, −5.45, −5.06, and −5.62 kcal/mol, respectively. These values were markedly higher than the binding affinity of the control compound, Diclofenac, which showed a binding affinity of −4.52 kcal/mol (Table 4).

2D and 3D interactions of the selected compounds with the targeted receptor.

Post-docking analyses of the three most promising compounds revealed various chemical interactions, including H-bonds, hydrophilic bonds, and other interactions, as shown in Table 5 and Fig. 10. CID 72276 demonstrated various interactions with the COX-2 receptor by forming four hydrogen bonds with LYS83, ARG120, SER119, and GLU524, along with additional interactions involving VAL89, PRO86, LEU93, ILE112, TYR115, VAL116, LEU123, TYR355, PHE470, MET471, and LEU472 amino acid residues, as represented in Fig. 10 (A). Fig. 10 (B) illustrates the interaction of CID 5280343 with the COX-2 receptor, highlighting hydrogen bond formation with ARG120 and GLU524, as well as additional interactions with amino acid residues including LYS83, VAL89, PRO86, LEU93, TYR115, ILE112, VAL116, SER119, LEU123, TYR355, and MET471. The control molecule CID 3033 formed two hydrogen bonds with ARG513 and HIE90, three hydrophilic bonds with GLN192, SER353, and SER530, and additional interactions with ARG120, LEU352, TYR348, VAL349, LEU359, TYR355, LEU384, TRP387, TYR385, ALA516, PHE518, ILE517, MET522, GLY526, ALA527, VAL523, and LEU531 amino acid residues upon interacting with the COX-2 protein, as depicted in Fig. 10 (C).

3.11.2. ADME and toxicity analysis of the identified compounds

The pharmacokinetic properties of a compound should be determined before considering it as a possible drug candidate [70]. Lipinski's rule of five is a useful tool for assessing the drug-like properties of compounds. The following parameters are considered: (i) molar refractivity between 40 and 130; (ii) Lipophilicity <5; (iii) H-bond donors ≤5; (iv) H-bond acceptors ≤10; and (v) molecular weight <500. According to Veber's and Lipinski's rule of five, all the selected molecules are suitable for developing new drugs. Apart from pharmacokinetics properties, these two compounds also provide good toxicological confirmation, as depicted in Table 6.

3.11.3. MD simulation study

MD simulation is a useful tool for checking how stable the structures of protein-ligand complexes are over a certain amount of time in a synthetic macromolecular environment [71]. RMSD, RMSF, SASA, and Rg are important measurements used in MD simulations that give a full picture of how protein-ligand complexes behave at the molecular level. We conducted a 100 ns simulation for apo-proteins and their corresponding complexes.

3.11.3.1. RMSD analysis of protein-ligand complexes. The RMSD analysis was carried out to assess the average fluctuations generated by dislocating an atom during a particular time scale [72]. A reference frame backbone was initially aligned with protein frames during MD simulations. RMSD was calculated by selecting atoms from the system. The compounds CID 72276, and CID 5280343 in complex with COX-2 showed average Cα-RMSD values of 2.39 Å, and 2.66 Å, accordingly, while CID 3033 (control) and apo (5KIR) exhibited average Cα-RMSD values of 2.36 Å, and 3.30 Å that represent the structural stability of two lead compounds compared to apo (5KIR) and maintained stable trajectories throughout the simulation period. The complex involving CID 5280343 displayed minor fluctuations from 23 ns to 100 ns, the highest peaking at 3.40 Å even though it is not more than apo (5KIR). The remaining complex showed no fluctuation throughout the simulation runtime, as presented in Fig. 11.

3.11.3.2. RMSF analysis of protein-ligand complexes. RMSF calculates the average difference between atomic residual positions and their mean positions in MD simulations over time [73]. It is also used for protein characterization, which examines protein flexibility

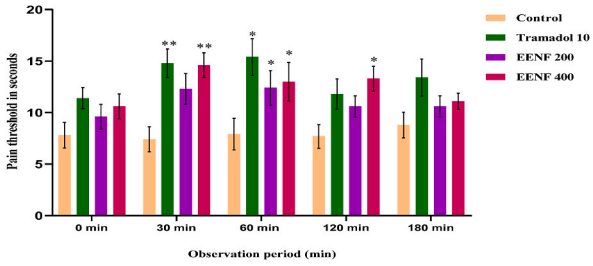

Fig. 8. Effects of EENF in the hot plate study in mice (n = 5) are presented as mean ± SEM. Comparisons with the control group indicated statistical significance at ***p < 0.001, **p < 0.01, and *p < 0.05.

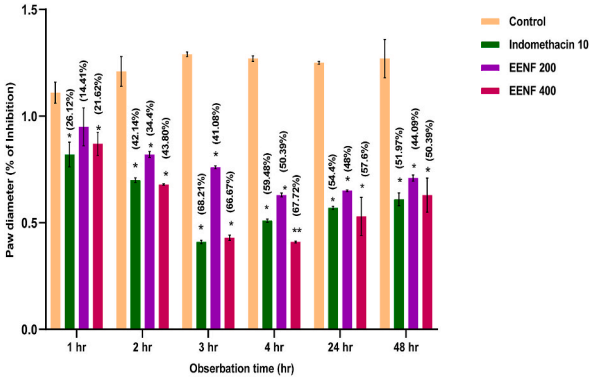

Fig. 9. Percentage of edema inhibition by EENF in formalin-induced paw edema in mice is presented as mean ± SEM. Comparisons with the control group revealed statistical significance at ***p < 0.001, **p < 0.01, and *p < 0.05.

Table 4
Docking scores for the identified compounds.

SN	PubChem ID	Phytochemical name	Docking scores (Kcal/mol)
1.	CID 72276	(−) Epicatechin	−8.62
2.	CID 5280343	Quercetin	−8.59
3.	CID 5280863	Kaempferol	−7.69
4.	CID 5281672	Myricetin	−5.82
5.	CID 5281792	Rosmarinic acid	−5.74
6.	CID 2802516	1,5-diphenyl-2h-1,2,4-triazoline-3-thione	−5.49
7.	CID 5363867	2,3-dehydro-4-oxo-.beta.-ionone	−5.45
8.	CID 444539	trans-Cinnamic acid	−5.06
9.	CID 689043	Caffeic acid	−5.62
10.	CID 3033 (control)	Diclofenac	−4.52

Table 5
An analysis of the binding interaction between the top two compounds and the reference compound (diclofenac) against the COX-2 protein.

Protein name	(Ligand) PubChem ID	H-bonds	Hydrophilic bonds	Other bonds
COX-2	CID 72276	LYS83, ARG120, SER119, GLU524	SER119	VAL89, PRO86, LEU93, ILE112, TYR115, VAL116, LEU123, TYR355, PHE470, MET471, LEU472
	CID 5280343	ARG120, GLU524	SER119	LYS83, PRO86, VAL89, LEU93, ILE112, TYR115, VAL116, LEU123, TYR355, MET471
	CID 3033 (Control)	ARG513, HIE90	GLN192, SER353, SER530	ARG120, LEU352, TYR348, VAL349, TYR355, LEU359, LEU384, TYR385, TRP387, ALA516, ILE517, PHE518, MET522, VAL523, GLY526, ALA527, LEU531

throughout the simulation run. RMSF plot studies of all the protein-ligand complexes are shown in Fig. 12. The RMSF trajectories of CID 72276, and CID 5280343 for COX-2 were calculated compared to the control compound CID 3033, and Apo protein (5KIR). The average RMSF values for CID 72276, and CID 5280343 in complex with COX-2 were 1.04 Å, and 1.19 Å, respectively, while the control compound CID 3033, and apo (5KIR) showed a 1.19 Å and 1.20 Å average RMSF value in complex with COX-2 which represents a minor fluctuation of COX-2 when it formed a complex with CID 72276, and CID 5280343. The RMSF trajectories of three protein-ligand complexes exhibited low RMSF values throughout the simulation runtime.

3.11.3.3. Rg analysis of protein-ligand complexes. Rg predicts a macromolecule's structural position, examines the atom distribution, and changes in compactness of the protein-ligand complex around its axis [74]. Research has demonstrated that a properly folded protein maintains a stable Rg. A lower Rg indicates a better compactness level. The average RG values for CID 72276 and CID 5280343 with COX-2 displayed an average of 3.90 Å and 4.06 Å, respectively. On the other hand, the control compound CID 3033-COX-2 complex exhibited an average RG of 3.45 Å, which is nearer to the two lead compounds, indicating better compactness of the protein-ligand complex around its axis. Throughout the simulations, all protein complexes displayed a consistently stable trajectory with minor variations, as shown in Fig. 13.

3.11.3.4. SASA analysis of protein-ligand complexes. A greater SASA value indicates a relatively widened surface area [75]. An amino acid residue on the surface of a protein usually acts as an active site and interacts with other molecules. It assists to understand the

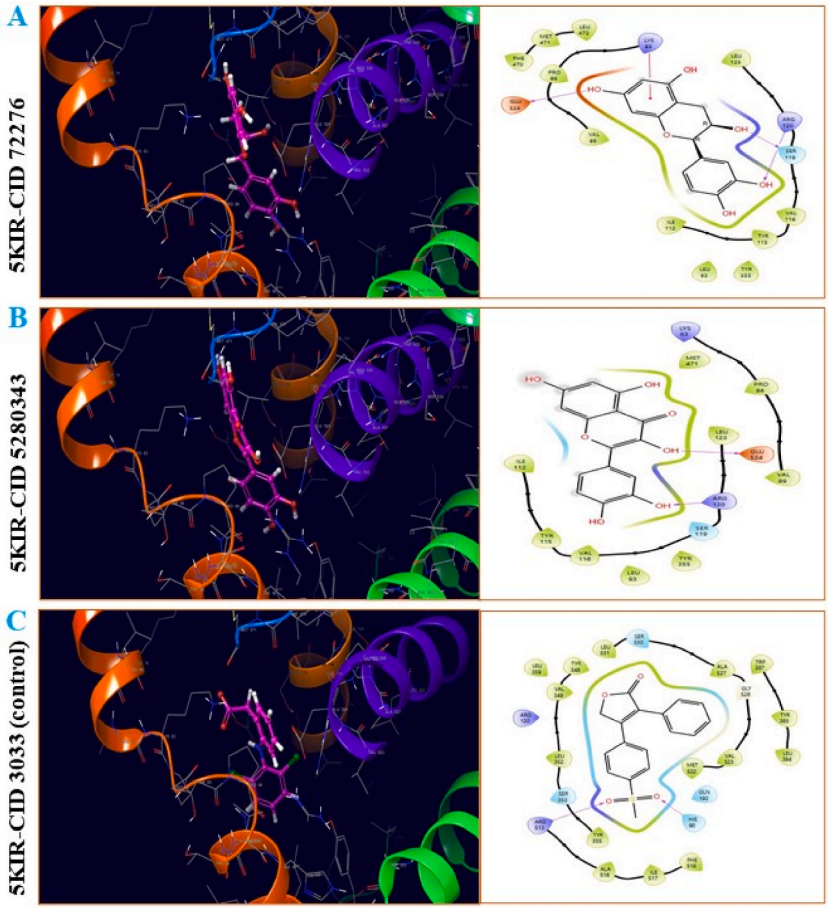

Fig. 10. Binding interactions of the top two phytochemicals along with control compounds with the COX-2 receptor. CID 72276, CID 5280343, and CID 3033 (control) are denoted by A, B, and C, respectively. On the left side, there's a 3D structure, while on the right side, there's a 2D structure of COX-2 binding complexes.

Table 6
Toxicity and pharmacokinetics properties of the selected compounds.

Ligand name (PubChem ID)		(−) Epicatechin (CID 72276)	Quercetin (CID 5280343)	(Diclofenac) CID 3033
Pharmacokinetics properties and toxicity	**MW**	290.271 g/mol	302.238 g/mol	296.15 g/mol
	NHA	6	7	2
	NHD	5	5	2
	Log P	0.85	1.23	4.36
	NRB	1	1	4
	GIA	High	High	High
	BBB	No	No	Yes
	HT	No	No	No
	AT	No	No	No
	CT	No	No	No
	NLV	0	0	0
	DL	Yes	Yes	Yes

MW-molecular weight (g/mol); NHD- No. of hydrogen bond donor; NHA- No. of hydrogen bond acceptor; LogP-Predicted octanol/water partition coefficient; NRB- No. of rotatable bonds; GIA-Gastrointestinal Absorption; BBB- Blood Brain Barrier; AT- AMES toxicity; HT- Hepatotoxicity; CT-Cytotoxicity; DL- Drug Likeness; NLV- Number of Lipinski's Violation.

compound or protein's solvent-like behavior (hydrophilic or hydrophobic). In COX-2 complexes, CID 72276 and CID 5280343 exhibited average SASA values of 82.38 Å2 and 327.93 A2, respectively. In contrast, the control CID 3033 had an average value of 132.97 Å2 when formed in a COX-2 complex. The CID 72276 complex with COX-2 demonstrated a relatively consistent SASA trajectory, characterized by minor fluctuations throughout the simulation runtime. This is lower than CID 3033, the control compound. As shown in Fig. 14, the CID 5280343-COX-2 complex changed a lot, which indicates that it has the widest surface area uncovered to the solvent.

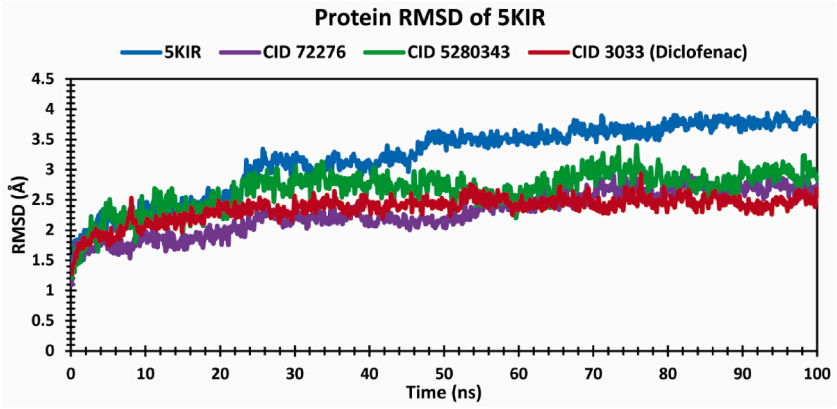

Fig. 11. Depicting the RMSD values of 5KIR (blue) CID 72276 (violet), CID 5280343 (green), CID 3033 (red), in a complex with COX-2 receptor, and over 100 ns simulation time scale.

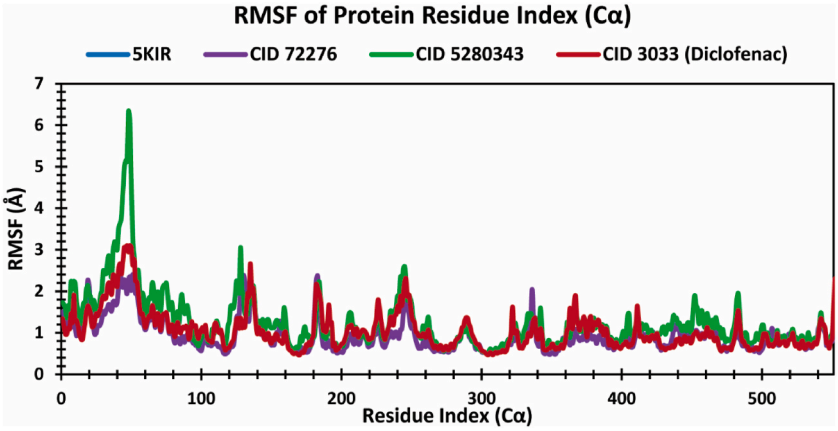

Fig. 12. Displaying the RMSF values collected from the protein in complex with CID 72276 (violet), CID 5280343 (green), and CID 3033 (red) ligands over a 100 ns simulation time scale.

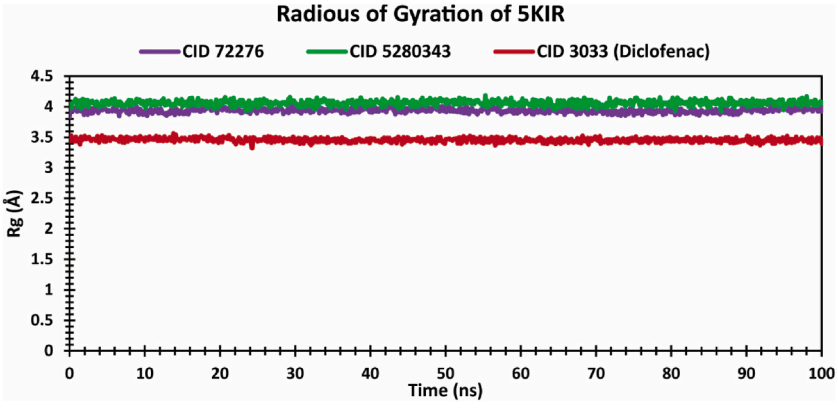

Fig. 13. The Rg value of the identified two compounds, CID 72276 (violet), and CID 5280343 (green), along with control CID 3033 (red), in complex with COX-2 over a 100 ns simulation period.

4. Discussion

Historically, plants are considered a principal origin of valuable therapeutic agents for treating various diseases [76]. Biomolecules from plants can offer new approaches to treating chronic illnesses in biological system, even in our modern age [77,78]. Biological activities are determined by the quantity of secondary metabolites in plant cells, which differs according to the seasons, climate, particular growth stages, plant parts, and extracting solvent. Leaves are one of the richest sources of bioactive molecules [79,80]. Current anti-inflammatory and analgesic drugs often lack long-term efficacy and carry significant side effects. In recent years, many researchers have explored alternative sources of drugs that appear to have fewer or no side effects. *N. fruticans*, is recognized for its abundance of polyphenols, flavonoids, vitamin E, protocatechuic acid, chlorogenic acid, kaempferol, and calcium and attracting interest for its many benefits [2,16,81]. Phytochemical screening of EENF revealed numerous types of constituents, including alkaloids, carbohydrates, tannins, glycosides, saponins, steroids, flavonoids, phenolic compounds, triterpenes, and gum, which have been documented for their antioxidant properties and other biological functions, namely anti-inflammatory effects. Furthermore, the experimental animals showed no mortality or abnormal behavior in the acute toxicity study, indicating the safety profile of the crude extract of *N. fruticans* used in the experiment.

HPLC analysis revealed that EENF contains a notably high level of (−)-epicatechin (36.32 ± 0.15 mg/100 g dry extract), while other phenolic compounds such as trans-cinnamic acid, rutin hydrate, quercetin, caffeic acid, kaempferol, myricetin, and rosmarinic acid were present in moderate to low amounts compared to a standard mixture of 16 polyphenolic compounds, as shown in Figs. 1 and 2. These findings, along with their significant pharmacological activities, are represented in Table 2. Additionally,15 identified phytochemicals of EENF via GC-MS, detailed in Table 3, with their pharmacological significance. Fig. 3 highlights three major compounds: 1-(hydroxymethyl)-1,2-ethanediyl ester (25.70 %), hexadecanoic acid (11.91 %), and L-(+)-ascorbic acid 2,6-dihexadecanoate (4.97 %), all of which possess antioxidant, analgesic, and anti-inflammatory properties. These findings represented the extract's complex phytochemical profile, which may contribute to its physiological activities, especially, its antioxidant and anti-inflammatory effect [82].

The analysis demonstrated EENF's substantial polyphenolic content, with a TPC of 239.87 ± 1.36 mg GAE/g dry extract, a TFC of 225 ± 1.13 mg QE/g dry extract, and a TTC of 103.70 ± 0.72 mg GAE/g dry extract, representing its rich antioxidant profile, which is crucial for reducing oxidative stress and eliminating free radicals. Their high reactivity with ROS helps mitigate cellular damage, potentially contributing to the prevention of various oxidative stress-related illnesses. In the DPPH free radical scavenging assay, EENF exhibited effective scavenging properties with an IC_{50} value of 105.18 μg/mL, in contrast to ascorbic acid, which had an IC_{50} value of 14.24 μg/mL, as shown in Fig. 4. The extract also showed significant reducing power with an RC_{50} value of 1752.76 μg/mL (Fig. 5). The identified antioxidant activities of phenolic compounds, flavonoids, and tannins are contributed to their capability to scavenge free radicals [83]. As a result, the antioxidant activity of the extract enhances its analgesic and anti-inflammatory potentials and suggests that EENF's multifaceted properties could offer a comprehensive approach to managing pain and inflammation.

In mice, acetic acid-induced abdominal contractions result in peripheral writhing in a brief period of time, and this behavior has been examined in mice to evaluate analgesic and anti-inflammatory remedies derived from plant [82] Intraperitoneal injection of acetic acid (0.7 %) elicits pain by facilitating the secretion of free arachidonic acid from tissue phospholipids via phospholipase A2 and acyl hydrolases. Arachidonic acid is subsequently shifted into prostaglandins, thromboxane, and prostacyclin through the cyclooxygenase pathway. The liberated prostaglandins, particularly prostaglandin E, and prostacyclin (PGI2), are accountable for the perception of localized pain. The frequency of writhing in mice was significantly reduced by the action of polyphenolic compounds, which alleviated pain and inflammation by inhibiting cyclooxygenase enzyme. A high dose of 400 mg/kg body weight of EENF resulted in an 80.07 % suppression of writhing, which is comparable to the 82.3 % suppression observed with the standard drug, suggesting that EENF exhibits a potent, dose-dependent analgesic effect (Fig. 6). The identified polyphenols and flavonoids of EENF (Figs. 1 and 2), particularly, rutin, quercetin, kaempferol, and luteolin, possess analgesic features by reducing the rate of writhing in

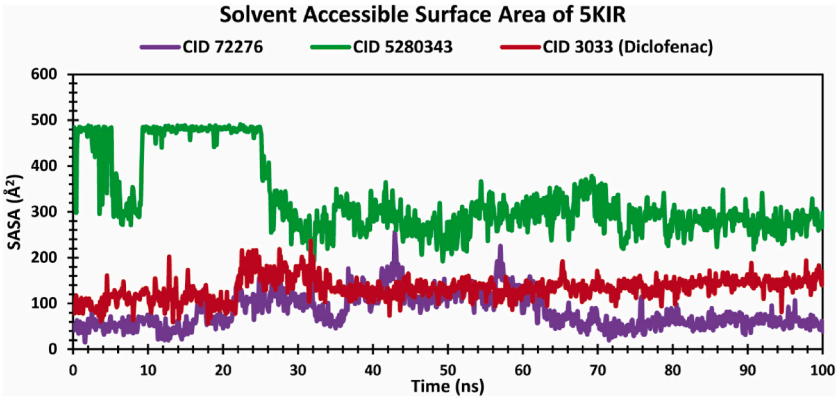

Fig. 14. Showing the SASA values of the protein-ligand complex over a 100 ns simulation period. The SASA values of the selected two compounds CID 72276 (violet), and CID 5280343 (green), along with control CID 3033 (red), in complex with COX-2.

mice through the suppression of prostaglandin synthesis [82,84].

The primary goal of the tail immersion model is to evaluate the effects of central analgesics in conjunction with opioid receptor agonists, which are particularly effective in this context. The analgesic effects of opioids involve both supraspinal (kappa-3, delta-1, and sigma-1) and spinal (kappa-1, delta-2, and sigma-2) receptors [85]. EENF showed a notable, time-dependent increase in latency, with the 400 mg/kg dose exhibiting the highest latency response at the 3rd observation period, illustrated in Fig. 7. Nonetheless, spinal and supraspinal reflexes are examined using the hot plate technique. It is also used for evaluating the mechanism of central analgesics, which are natural opioids. EENF at 400 mg/kg body weight produced a pronounced latency response, peaking at 120 min, demonstrating sustained analgesic activity (Fig. 8).

The inflammatory process is stimulated by higher production of ROS, advanced glycation end product, cytokines, prostaglandins, and nitric oxide (NO) [86]. Formalin-induced model is frequently employed to assess the *in vivo* anti-inflammatory efficacy of experimental plant' extract. This physiological phenomenon has 2 stages: the initial stage involves neurogenic consequences resulting from the activation of pain receptors, while the subsequent stage is characterized by anti-inflammatory responses influenced by peripheral inflammation mediated via prostaglandin-like chemical agents. This study depicted that the extract inhibits all stages of inflammation, with the most significant impact observed. EENF showed the highest inhibition of edema at the fourth hour, with 50.39 % and 67.72 % inhibition observed at doses of 200 and 400 mg/kg body weight, respectively, following formalin administration. In contrast, the standard drug showed its maximum response (68.21 % inhibition) at the third hour (Fig. 9). However, it also markedly lowered inflammation at both 24 h and 48 h following formalin administration as illustrated in Fig. 9. Therefore, the extract may inhibit the first and subsequent phases of inflammation through obstructing the activity of pro-inflammatory mediators and cyclooxygenase enzyme, accordingly [82]. This indicates that EENF not only provides substantial analgesic effects but also efficiently reduces inflammation, outperforming the standard drug, Indomethacin, across all tested doses.

The extract could possess potent antioxidant, analgesic, and anti-inflammatory properties due to its polyphenols and flavonoids, which have been reported to reduce ROS level and block macrophage-mediated cytokine production. Moreover, these bioactive compounds also inhibit the COX-2 enzyme, similar to NSAIDs including tramadol, ibuprofen, and diclofenac sodium, which were utilized as reference drugs in the *in-vivo* investigation. Nowadays, the computational drug design approach is widely used to predict how novel drug compounds may impact various diseases using advanced computational techniques. Researchers can utilize computer-simulated environments for drug discovery and development, reducing the need for costly and time-consuming laboratory tests. In molecular docking, a key and lock approach were employed in order to determine complicated protein–ligand complexes having the greatest binding affinities [87].

Molecular docking study revealed that nine ligands from the GC-MS and HPLC analyses exhibited strong binding affinities with the COX-2 receptor, with CID 72276 and CID 5280343 showing the highest binding scores of −8.62 and −8.59 kcal/mol, correspondingly, surpassing Diclofenac (−4.52 kcal/mol) (Table 4). Detailed 2D and 3D interaction analyses [Fig. 10(A–C)] highlighted that these two lead compounds form multiple hydrogen bonds and additional relations with key amino acid residues of the COX-2 receptor, potentially contributing to their high binding affinities. Based on the outcomes of the molecular docking analysis and their ADMET profiles, they were selected for molecular dynamics simulation (MDS). MDS have become an essential tool for computer-aided design that analyzes the movements of atoms and gives a sense of the protein-ligand interaction's stability. Moreover, it may verify the rigidity and stability of protein-ligand complexes under the body's most extreme circumstances [88]. The Cα-RMSD explains the overall stability of the proteins and their complexes in a biological system where higher values indicate more significant deviations from the starting structure [89].

MD simulations assessed the stability of these interactions over time, showing that CID 72276 and CID 5280343 maintained stable trajectories with average RMSD values of 2.39 Å and 2.66 Å, respectively (Fig. 11). Rg analysis demonstrates the overall compactness and conformational stability of protein-ligand complexes. A high degree of compactness is indicated by a lessen Rg value, while a disassociation of the chemicals from the protein is indicated by a higher value [90]. The compactness of the protein-ligand complexes, marked by lower Rg values for CID 72276 and CID 5280343, supports their stable binding (Fig. 13). Additionally, SASA analysis suggested that while CID 5280343 exhibited the most surface area exposure, CID 72276 demonstrated consistent SASA values, reinforcing their effective binding and potential for therapeutic development (Fig. 14). The study did not investigate the molecular mechanisms of the *in-silico* analysis outcomes, which are needed to be coalesced with *in vivo* evidences. Consequently, further investigation is needed to figure out the exact mode of action of the extract and to emphasize the significant bioactive compounds essential to their anti-nociceptive and anti-inflammatory activities, in order to develop novel plant-based drugs [87].

5. Conclusion

The current research demonstrates that the *Nypa fruticans* extract exhibits significant pain inhibiting effects, peripheral anti-nociceptive effects, and anti-inflammatory properties in mice. HPLC and GC-MS chemical profiling identified 23 phytochemicals, with (−) epicatechin and quercetin being the most prominent bioactive components in the studied extract. We postulate that both of these compounds could be employed as templates for developing novel, safe, and efficient anti-inflammatory drugs by inhibiting COX-2 enzyme, similar to standard NSAIDs. Additionally, the *in-vitro* tests, the experimental analgesic, and anti-inflammatory activities, along with the computer-based molecular docking studies provide significant scientific support for validating the traditional medicinal applications of *N. fruticans*. According to research findings, *Nypa fruticans* is suggested as a supplementary and complementary treatment for inflammatory illnesses, highlighting its potential values. However, future investigations, including pure compounds isolation and their safety profile, comprehensive preclinical study with safety data, validation through appropriate human trials, advanced *in vivo* studies related to the mechanisms of action, and biomolecular studies, are required to corroborate these findings.

CRediT authorship contribution statement

Farhana Islam: Writing – review & editing, Writing – original draft, Visualization, Validation, Software, Resources, Project administration, Methodology, Investigation, Funding acquisition, Formal analysis, Data curation, Conceptualization. **Md. Aktaruzzaman:** Writing – review & editing, Visualization, Validation, Software, Investigation, Formal analysis, Data curation. **Md. Tarikul Islam:** Writing – review & editing, Visualization, Validation, Software, Investigation, Formal analysis, Data curation. **Fariya Islam Rodru:** Visualization, Validation, Software, Formal analysis. **Saquiba Yesmine:** Writing – review & editing, Validation, Supervision, Project administration, Methodology.

Ethics declarations

All the *in-vivo* experimental procedures were performed by the guidelines of the Biosafety, Biosecurity, and Ethical Committee of Jahangirnagar University **[Ref No: BBEC, JU/M 2023/11 (68)] .**

Data availability statement

Data will be made available upon request.

Declaration of competing interest

The authors declare that they have no known competing financial interests or personal relationships that could have appeared to influence the work reported in this paper.

Acknowledgments

The authors express their gratitude to the dept. of pharmacy, Jashore University of Science and Technology, and the pharmacology laboratory of Jahangirnagar University, Savar, Dhaka, Bangladesh, for providing experimental mice and offering sufficient assistance in conducting the research work.

References

[1] J. Zhang, Y. Wu, C. Wang, W. Xu, Z. Zhang, S. Zhang, X. Guan, X. Wang, The antioxidant, anti-inflammatory and analgesic activity effect of ethyl acetate extract from the flowers of Syringa pubescens Turcz, J. Ethnopharmacol. 322 (2024) 117561, https://doi.org/10.1016/j.jep.2023.117561.
[2] H. Park, T. Jang, S. Han, S. Oh, J. Lee, S. Myoung, J. Park, Anti-inflammatory effects of Nypa fruticans Wurmb via NF-κB and MAPK signaling pathways in macrophages, Exp. Ther. Med. 24 (2022), https://doi.org/10.3892/etm.2022.11690.
[3] T. Liu, L. Zhang, D. Joo, S.C. Sun, NF-κB signaling in inflammation, Signal Transduct. Targeted Ther. 2 (2017), https://doi.org/10.1038/sigtrans.2017.23.
[4] L. Chen, H. Deng, H. Cui, J. Fang, Z. Zuo, J. Deng, Y. Li, X. Wang, L. Zhao, Inflammatory responses and inflammation-associated diseases in organs, Oncotarget 9 (6) (2017) 7204.
[5] A. Jalali, F. Dabaghian, H. Akbrialiabad, F. Foroughinia, M.M. Zarshenas, A pharmacology-based comprehensive review on medicinal plants and phytoactive constituents possibly effective in the management of COVID-19, Phytother Res. 35 (2021) 1925–1938, https://doi.org/10.1002/PTR.6936.
[6] F. Li, J. Huo, Y. Zhuang, H. Xiao, W. Wang, L. Huang, Anti-nociceptive and anti-inflammatory effects of the ethanol extract of Arenga pinnata (Wurmb) Merr. fruit, J. Ethnopharmacol. 248 (2020), https://doi.org/10.1016/j.jep.2019.112349.
[7] G. Pizzino, N. Irrera, M. Cucinotta, G. Pallio, F. Mannino, V. Arcoraci, F. Squadrito, D. Altavilla, A. Bitto, Oxidative stress: harms and benefits for human health, Oxid. Med. Cell. Longev. 2017 (2017), https://doi.org/10.1155/2017/8416763.
[8] K. Sobhani, J. Li, M. Cortes, Nonsteroidal anti-inflammatory drugs (NSAIDs), First Aid Perioperative Ultrasound: Acute Pain Manual for Surgical Procedures (2023) 127–138, https://doi.org/10.1007/978-3-031-21291-8_8.
[9] G. Di Maio, I. Villano, C.R. Ilardi, A. Messina, V. Monda, A.C. Iodice, C. Porro, M.A. Panaro, S. Chieffi, G. Messina, M. Monda, M. La Marra, Mechanisms of transmission and processing of pain: a narrative review, Int. J. Environ. Res. Publ. Health 20 (2023), https://doi.org/10.3390/ijerph20043064.
[10] E. Ricciotti, G.A. Fitzgerald, Prostaglandins and inflammation, Arterioscler. Thromb. Vasc. Biol. 31 (2011) 986–1000, https://doi.org/10.1161/ATVBAHA.110.207449.
[11] A. Zarghi, S. Arfaei, Selective COX-2 Inhibitors: A Review of Their Structure-Activity Relationships, 2011.
[12] C.L. Gorlenko, H.Y. Kiselev, E.V. Budanova, A.A. Zamyatnin, L.N. Ikryannikova, Plant secondary metabolites in the battle of drugs and drug-resistant bacteria: new heroes or worse clones of antibiotics? Antibiotics 9 (2020) https://doi.org/10.3390/antibiotics9040170.
[13] S. Rudra, K.N. Islam, M.M. Rahman, S.B. Uddin, Medicinal plant diversity and their therapeutic uses in selected village common forests in chittagong hill tracts, Bangladesh, J. Herbs, Spices, Med. Plants (2021) 1–25, https://doi.org/10.1080/10496475.2020.1786874.
[14] PharmacologyOnLine | Front, (n.d.). https://pharmacologyonline.silae.it/front (accessed December 17, 2024).
[15] B. Biswas, M. Golder, T. Islam, S.K. Sadhu, Comparative antioxidative and antihyperglycemic profiles of pneumatophores of two mangrove species Avicennia alba and Sonneratia apetala, Dhaka Univ. J. Pharm. Sci. 17 (2018) 205–211, https://doi.org/10.3329/dujps.v17i2.39177.
[16] Md Farid Hossain, Utilization of mangrove forest plant: nipa palm (Nypa fruticans wurmb.), Am. J. Agric. For. 3 (2015) 156, https://doi.org/10.11648/j.ajaf.20150304.16.
[17] N. Prasad, B. Yang, K.W. Kong, H.E. Khoo, J. Sun, A. Azlan, A. Ismail, Z. Bin Romli, Phytochemicals and antioxidant capacity from Nypa fruticans Wurmb. Fruit, Evid. base Compl. Alternative Med. 2013 (2013), https://doi.org/10.1155/2013/154606.
[18] N.A. Yusoff, M.F. Yam, H.K. Beh, K.N. Abdul Razak, T. Widyawati, R. Mahmud, M. Ahmad, M.Z. Asmawi, Antidiabetic and antioxidant activities of Nypa fruticans Wurmb. vinegar sample from Malaysia, Asian Pac. J. Tropical Med. 8 (2015) 595–605, https://doi.org/10.1016/j.apjtm.2015.07.015.
[19] G.D. Nugroho, M.F. Wiraatmaja, P.S. Pramadaningtyas, S. Febriyanti, N. Liza, D.M.D. Naim, Y.I. Ulumuddin, A.D. Setyawan, Review: phytochemical composition, medicinal uses and other utilization of Nypa fruticans, International Journal of Bonorowo Wetlands 10 (2022), https://doi.org/10.13057/bonorowo/w100105.
[20] K.K. Sarkar, T. Mitra, M.A. Rahman, I.M. Raja, M. Aktaruzzaman, M.A. Abid, M.N.H. Zilani, D.N. Roy, In vivo bioactivities of Hoya parasitica (wall.) and in silico study against cyclooxygenase enzymes, BioMed Res. Int. 2022 (2022), https://doi.org/10.1155/2022/1331758.

[21] S. Biswas, D. Mondol, P. Jodder, S. Sana, MdA. Saleh, A.K. Tarafdar, F. Islam, Evaluation of neurobehavioral activities of ethanolic extract of Psidium guajava Linn leaves in mice model, Futur J Pharm Sci 7 (2021) 36, https://doi.org/10.1186/s43094-021-00188-5.

[22] K.K. Sarkar, T. Mitra, M. Aktaruzzaman, M.A. Abid, M.A. Rahman, P. Debnath, S.K. Sadhu, Exploring antioxidative, cytotoxic and neuropharmacological insights into Bixa orellana leaves: experimental and in silico approaches, Heliyon 10 (2024) e27001, https://doi.org/10.1016/j.heliyon.2024.e27001.

[23] M.M. Medha, H.S. Devnath, B. Biswas, B. Bokshi, S.K. Sadhu, In silico profiling of analgesic and antihyperglycemic effects of ethanolic leaves extract of Amischotolype mollissima: evidence from in vivo studies, Saudi J. Biol. Sci. 29 (2022) 103312, https://doi.org/10.1016/J.SJBS.2022.103312.

[24] M.J. Uddin, Md Mohaimenul, Md Aktaruzzaman, MdT. Islam, R.H. Al, MdH. Rahman, T. Akter, MdM. Rahman, MdZ. Amin, MdO. Raihan, Isolation and quantification of caffeine in marketed tea and carbonated beverage products in Bangladesh, Toxicologie Analytique et Clinique 4481 (2024) 1, https://doi.org/10.1016/j.toxac.2024.09.001.

[25] N. Nahar, M. Nazmul Hasan Zilani, P. Biswas, M. Morsaline Billah, S. Bibi, N.A. Albekairi, A. Alshammari, M. Nazmul Hasan, Profiling of secondary metabolite and evaluation of anti-diabetic potency of Crotalaria quinquefolia (L): in-vitro, in-vivo, and in-silico approaches, Saudi Pharmaceut. J. 32 (2024), https://doi.org/10.1016/j.jsps.2023.101887.

[26] S. Rahman, N.H. Zilani, A. Islam, M. Hasan, in: In Vivo Neuropharmacological Potential of, 2021.

[27] S. Akhter, MdW. Hossain, S. Sultana, J. Ferdous Jharna, N. Sultana Meghla, R. Alam, K.M. Anis-Ul-Haque, Md Mashiar Rahman, Ruellia prostrata Poir. activity evaluated by phytoconstituents, antioxidant, anti-inflammatory, antibacterial activity, and in silico molecular functions, J. Saudi Chem. Soc. 26 (2022) 101401, https://doi.org/10.1016/j.jscs.2021.101401.

[28] S.C. Sahu, L. Navarro, A.W. Hayes, Toxicity, acute, in: P. Wexler (Ed.), Encyclopedia of Toxicology, fourth ed.), fourth ed., Academic Press, Oxford, 2024, pp. 409–419, https://doi.org/10.1016/B978-0-12-824315-2.00607-2.

[29] K.K. Sarkar, T. Mitra, M.A. Rahman, I.M. Raja, M. Aktaruzzaman, M.A. Abid, M.N.H. Zilani, D.N. Roy, In vivo bioactivities of Hoya parasitica (wall.) and in silico study against cyclooxygenase enzymes, BioMed Res. Int. 2022 (2022), https://doi.org/10.1155/2022/1331758.

[30] R.A. Moushome, M.I. Akter, M.A. Aziz, Phytochemical screening and antinociceptive and antidiarrheal activities of hydromethanol and petroleum benzene extract of microcos paniculata barks, BioMed Res. Int. 2016 (2016) 3167085, https://doi.org/10.1155/2016/3167085.

[31] T. Kumar, V. Jain, Antinociceptive and anti-inflammatory activities of bridelia retusa methanolic fruit extract in experimental animals, Sci. World J. 2014 (2014), https://doi.org/10.1155/2014/890151.

[32] R.A. Friesner, R.B. Murphy, M.P. Repasky, L.L. Frye, J.R. Greenwood, T.A. Halgren, P.C. Sanschagrin, D.T. Mainz, Extra precision glide: docking and scoring incorporating a model of hydrophobic enclosure for protein-ligand complexes, J. Med. Chem. 49 (2006) 6177–6196, https://doi.org/10.1021/jm051256o.

[33] S.W. Rowlinson, J.R. Kiefer, J.J. Prusakiewicz, J.L. Pawlitz, K.R. Kozak, A.S. Kalgutkar, W.C. Stallings, R.G. Kurumbail, L.J. Marnett, A novel mechanism of cyclooxygenase-2 inhibition involving interactions with ser-530 and tyr-385, J. Biol. Chem. 278 (2003) 45763–45769, https://doi.org/10.1074/jbc.M305481200.

[34] Z. Orgován, G.G. Ferenczy, G.M. Keserű, The role of water and protein flexibility in the structure-based virtual screening of allosteric GPCR modulators: an mGlu 5 receptor case study, J. Comput. Aided Mol. Des. 33 (2019) 787–797.

[35] K. Roos, C. Wu, W. Damm, M. Reboul, J.M. Stevenson, C. Lu, M.K. Dahlgren, S. Mondal, W. Chen, L. Wang, R. Abel, R.A. Friesner, E.D. Harder, OPLS3e: Extending Force Field Coverage for Drug-Like Small Molecules, J. Chem. Theor. Comput. 15 (2019) 1863–1874, https://doi.org/10.1021/acs.jctc.8b01026.

[36] P.C. Agu, C.A. Afiukwa, O.U. Orji, E.M. Ezeh, I.H. Ofoke, C.O. Ogbu, E.I. Ugwuja, P.M. Aja, Molecular docking as a tool for the discovery of molecular targets of nutraceuticals in diseases management, Sci. Rep. 13 (2023) 1–18, https://doi.org/10.1038/s41598-023-40160-2.

[37] MdE.K. Talukder, MdF. Atif, N.H. Siddiquee, S. Rahman, N.I. Rafi, S. Israt, N.F. Shahir, MdT. Islam, A. Samad, T.A. Wani, MdM. Rahman, F. Ahammad, Molecular docking, QSAR, and simulation analyses of EGFR-targeting phytochemicals in non-small cell lung cancer, J. Mol. Struct. 1321 (2025) 139924, https://doi.org/10.1016/j.molstruc.2024.139924.

[38] MdT. Islam, Md Aktaruzzaman, A. Saif, A.R. Hasan, MdM.H. Sourov, B. Sikdar, S. Rehman, A. Tabassum, S. Abeed-Ul-Haque, M.H. Sakib, MdM.A. Muhib, MdA. A. Setu, F. Tasnim, R. Rayhan, M.M. Abdel-Daim, MdO. Raihan, Identification of acetylcholinesterase inhibitors from traditional medicinal plants for Alzheimer's disease using *in silico* and machine learning approaches, RSC Adv. 14 (2024) 34620–34636, https://doi.org/10.1039/D4RA05073H.

[39] E. Harder, W. Damm, J. Maple, C. Wu, M. Reboul, J.Y. Xiang, L. Wang, D. Lupyan, M.K. Dahlgren, J.L. Knight, J.W. Kaus, D.S. Cerutti, G. Krilov, W.L. Jorgensen, R. Abel, R.A. Friesner, OPLS3: a force field providing broad coverage of drug-like small molecules and proteins, J. Chem. Theor. Comput. 12 (2016) 281–296, https://doi.org/10.1021/acs.jctc.5b00864.

[40] S.W. Rowlinson, J.R. Kiefer, J.J. Prusakiewicz, J.L. Pawlitz, K.R. Kozak, A.S. Kalgutkar, W.C. Stallings, R.G. Kurumbail, L.J. Marnett, A novel mechanism of cyclooxygenase-2 inhibition involving interactions with ser-530 and tyr-385, J. Biol. Chem. 278 (2003) 45763–45769, https://doi.org/10.1074/jbc.M305481200.

[41] G. Biala, E. Kedzierska, M. Kruk-Slomka, J. Orzelska-Gorka, S. Hmaidan, A. Skrok, J. Kaminski, E. Havrankova, D. Nadaska, I. Malik, Research in the field of drug design and development, Pharmaceuticals 16 (2023), https://doi.org/10.3390/ph16091283.

[42] A. Daina, O. Michielin, V. Zoete, SwissADME: a free web tool to evaluate pharmacokinetics, drug-likeness and medicinal chemistry friendliness of small molecules, Sci. Rep. 7 (2017) 1–13, https://doi.org/10.1038/srep42717.

[43] P. Banerjee, A.O. Eckert, A.K. Schrey, R. Preissner, ProTox-II: a webserver for the prediction of toxicity of chemicals, Nucleic Acids Res. 46 (2018) W257–W263, https://doi.org/10.1093/nar/gky318.

[44] S. Singh, Q. Bani Baker, D.B. Singh, Chapter 18 - molecular docking and molecular dynamics simulation, in: D.B. Singh, R.K. Pathak (Eds.), Bioinformatics, Academic Press, 2022, pp. 291–304, https://doi.org/10.1016/B978-0-323-89775-4.00014-6.

[45] F.A.D.M. Opo, M.M. Rahman, F. Ahammad, I. Ahmed, M.A. Bhuiyan, A.M. Asiri, Structure based pharmacophore modeling, virtual screening, molecular docking and ADMET approaches for identification of natural anti-cancer agents targeting XIAP protein, Sci. Rep. 11 (2021) 1–18, https://doi.org/10.1038/s41598-021-83626-x.

[46] E.J. Carrillo-Martinez, F.Y. Flores-Hernández, A.M. Salazar-Montes, H.F. Nario-Chaidez, L.D. Hernández-Ortega, Quercetin, a flavonoid with great pharmacological capacity, Molecules 29 (2024), https://doi.org/10.3390/molecules29051000.

[47] K.M. Monteiro Espíndola, R.G. Ferreira, L.E. Mosquera Narvaez, A.C. Rocha Silva Rosario, A.H. Machado Da Silva, A.G. Bispo Silva, A.P. Oliveira Vieira, M. Chagas Monteiro, Chemical and pharmacological aspects of caffeic acid and its activity in hepatocarcinoma, Front. Oncol. 9 (2019), https://doi.org/10.3389/fonc.2019.00541.

[48] A. Ganeshpurkar, A.K. Saluja, The pharmacological potential of rutin, Saudi Pharmaceut. J. 25 (2017) 149–164, https://doi.org/10.1016/j.jsps.2016.04.025.

[49] S. Parvizpour, Y. Masoudi-Sobhanzadeh, M.M. Pourseif, A. Barzegari, J. Razmara, Y. Omidi, Pharmacoinformatics-based phytochemical screening for anticancer impacts of yellow sweet clover, Melilotus officinalis (Linn.) Pall, Comput. Biol. Med. 138 (2021) 104921, https://doi.org/10.1016/j.compbiomed.2021.104921.

[50] MdK. Azhar, S. Anwar, G.M. Hasan, A. Shamsi, A. Islam, S. Parvez, MdI. Hassan, Comprehensive insights into biological roles of rosmarinic acid: implications in diabetes, Cancer and Neurodegenerative Diseases, Nutrients 15 (2023), https://doi.org/10.3390/nu15194297.

[51] Y. Taheri, H.A.R. Suleria, N. Martins, O. Sytar, A. Beyatli, B. Yeskaliyeva, G. Seitimova, B. Salehi, P. Semwal, S. Painuli, A. Kumar, E. Azzini, M. Martorell, W. N. Setzer, A. Maroyi, J. Sharifi-Rad, Myricetin bioactive effects: moving from preclinical evidence to potential clinical applications, BMC Complement Med Ther 20 (2020) 241, https://doi.org/10.1186/s12906-020-03033-z.

[52] D.K. Semwal, R.B. Semwal, S. Combrinck, A. Viljoen, Myricetin: a dietary molecule with diverse biological activities, Nutrients 8 (2016), https://doi.org/10.3390/nu8020090.

[53] A.V. Anand David, R. Arulmoli, S. Parasuraman, Overviews of biological importance of quercetin: a bioactive flavonoid, Phcog. Rev. 10 (2016) 84–89, https://doi.org/10.4103/0973-7847.194044.

[54] A. Bułakowska, J. Sławiński, R. Hałasa, A. Hering, M. Gucwa, J.R. Ochocka, J. Stefanowicz-Hajduk, An in vitro antimicrobial, anticancer and antioxidant activity of N–[(2–Arylmethylthio)phenylsulfonyl]cinnamamide derivatives, Molecules 28 (2023), https://doi.org/10.3390/molecules28073087.

[55] N. Ruwizhi, B.A. Aderibigbe, Cinnamic acid derivatives and their biological efficacy, Int. J. Mol. Sci. 21 (2020), https://doi.org/10.3390/ijms21165712.

[56] N. Sultana, H.J. Chung, N.U. Emon, S. Alam, M.T.I. Taki, S. Rudra, A. Tahamina, R. Alam, F. Ahmed, A. Al Mamun, Biological functions of Dillenia pentagyna roxb. Against pain, inflammation, fever, diarrhea, and thrombosis: evidenced from in vitro, in vivo, and molecular docking study, Front. Nutr. 9 (2022), https://doi.org/10.3389/fnut.2022.911274.

[57] M. Yang, J. Luo, K. Li, S. Hu, T. Ding, H. Liu, P. Sheng, M. Yang, Determination and pharmacokinetic study of guaiol in rat plasma by gas chromatography–mass spectrometry with selected ion monitoring, J. Chromatogr. B 1085 (2018) 30–35, https://doi.org/10.1016/j.jchromb.2018.03.041.

[58] Z. Song, F. Yin, B. Xiang, B. Lan, S. Cheng, Systems pharmacological approach to investigate the mechanism of acori tatarinowii rhizoma for Alzheimer's disease, Evid. base Compl. Alternative Med. 2018 (2018), https://doi.org/10.1155/2018/5194016.

[59] X. Yan, J. Lin, Z. Liu, S.D. David, D. Liang, S. Nie, M. Ge, Z. Xue, W. Li, J. Qiao, The recent progress of tricyclic aromadendrene-type sesquiterpenoids: biological activities and biosynthesis, Biomolecules 14 (2024), https://doi.org/10.3390/biom14091133.

[60] A. Paparella, L. Shaltiel-Harpaza, M. Ibdah, β-Ionone: its occurrence and biological function and metabolic engineering, Plants 10 (2021), https://doi.org/10.3390/plants10040754.

[61] M.L. Gonzalez-Rivera, J.C. Barragan-Galvez, D. Gasca-Martínez, S. Hidalgo-Figueroa, M. Isiordia-Espinoza, A.J. Alonso-Castro, In vivo neuropharmacological effects of neophytadiene, Molecules 28 (2023), https://doi.org/10.3390/molecules28083457.

[62] H. Ishtiaq, B. Ahmad, N. Zahid, T. Bibi, I. Khan, A. Azizullah, K. Ahmad, A. Murshed, S.U. Rehman, M.A. Abdel-Maksoud, M.A. El-Tayeb, J. Lu, M.Y. Zaky, Phytochemicals, antioxidant, and antidiabetic effects of ranunculus hirtellus aerial parts and roots: methanol and aqueous extracts, ACS Omega 9 (2024) 21805–21821, https://doi.org/10.1021/acsomega.3c08631.

[63] MdS. Rahman, MdN.H. Zilani, MdA. Islam, MdM. Hasan, MdM. Islam, F. Yasmin, P. Biswas, A. Hirashima, MdA. Rahman, MdN. Hasan, B. Kim, In vivo neuropharmacological potential of gomphandra tetrandra (wall.) sleumer and in-silico study against β-amyloid precursor protein, Processes 9 (2021), https://doi.org/10.3390/pr9081449.

[64] Ş.G. Küçükgüzel, P. Çıkla-Süzgün, Recent advances bioactive 1,2,4-triazole-3-thiones, Eur. J. Med. Chem. 97 (2015) 830–870, https://doi.org/10.1016/j.ejmech.2014.11.033.

[65] V. Kannan, R. Anandan, S. Srinivasan, N. Vijayasingh, Metabolites of docosahexaenoic acid produced by probiotic Bacillus cereus able to inhibit 2BX4 and 6LU7 receptors of SARS-COV-2. https://doi.org/10.15515/abr.0976-4585.13.5.183214, 2022.

[66] R. Kavitha, A.M. Uduman Mohideen, Identification of bioactive components and its biological activities of abelmoschas moschatus flower extrtact-A gc-ms study, IOSR Journal of Applied Chemistry (IOSR-JAC 10 (2017) 19–22, https://doi.org/10.9790/5736-1011011922.

[67] A. Mancini, E. Imperlini, E. Nigro, C. Montagnese, A. Daniele, S. Orrù, P. Buono, Biological and nutritional properties of palm oil and palmitic acid: effects on health, Molecules 20 (2015) 17339–17361, https://doi.org/10.3390/molecules200917339.

[68] L. Ralte, L. Khiangte, N.M. Thangjam, A. Kumar, Y.T. Singh, GC–MS and molecular docking analyses of phytochemicals from the underutilized plant, Parkia timoriana revealed candidate anti-cancerous and anti-inflammatory agents, Sci. Rep. 12 (2022) 3395, https://doi.org/10.1038/s41598-022-07320-2.

[69] R. Tripathi, V. Gupta, S. Tyagi, Hydroxymethyl ester derivative of hexadecanoic acid a possible hepatoprotectant from pulp of Cucurbita pepo, Indian J. Physiol. Allied Sci. 75 (2023) 59–60, https://doi.org/10.55184/ijpas.v75i04.208.

[70] D.K. Walker, The use of pharmacokinetic and pharmacodynamic data in the assessment of drug safety in early drug development, Br. J. Clin. Pharmacol. 58 (2004) 601–608, https://doi.org/10.1111/j.1365-2125.2004.02194.x.

[71] M.R. Challapa-Mamani, E. Tomás-Alvarado, A. Espinoza-Baigorria, D.A. León-Figueroa, R. Sah, A.J. Rodriguez-Morales, J.J. Barboza, Molecular docking and molecular dynamics simulations in related to leishmania donovani: an update and literature review, Trav. Med. Infect. Dis. 8 (2023), https://doi.org/10.3390/tropicalmed8100457.

[72] A. Samad, R. Alam, S. Hossen, K. Al-ghamdi, Calculations , and Molecular Dynamics Simulation Approaches, 2021.

[73] S.K. Paul, M. Saddam, K.A. Rahaman, J.G. Choi, S.S. Lee, M. Hasan, Molecular modeling, molecular dynamics simulation, and essential dynamics analysis of grancalcin: an upregulated biomarker in experimental autoimmune encephalomyelitis mice, Heliyon 8 (2022) e11232, https://doi.org/10.1016/j.heliyon.2022.e11232.

[74] A. Shrivastava, K. Mathur, R.K. Verma, S.K. Jayadev Magani, D.K. Vyas, A. Singh, Molecular dynamics study of tropical calcific pancreatitis (TCP) associated calcium-sensing receptor single nucleotide variation, Front. Mol. Biosci. 9 (2022) 982831, https://doi.org/10.3389/fmolb.2022.982831.

[75] S. Raphet, B. Javadi, Application of hierarchical clustering to analyze solvent-accessible surface area patterns in amycolatopsis lipases, Biology 11 (2022), https://doi.org/10.3390/biology11050652.

[76] F.E. Koehn, G.T. Carter, The evolving role of natural products in drug discovery, Nat. Rev. Drug Discov. 4 (2005) 206–220, https://doi.org/10.1038/nrd1657.

[77] K. Minogue, The explanatory model, Alien Powers (2018) 87–129, https://doi.org/10.4324/9781351321563-4.

[78] A.R. Hasan, F. Tasnim, Md Aktaruzzaman, MdT. Islam, R. Rayhan, A. Brishti, J. Hur, J.E. Porter, MdO. Raihan, The alteration of microglial calcium homeostasis in central nervous system disorders: a comprehensive review, Neuroglia 5 (2024) 410–444, https://doi.org/10.3390/neuroglia5040027.

[79] MdM. Nobee, A.R. Chowdhury, F.I. Rodru, J. Ahmed, H.K. Paul, K.K. Sarkar, F. Islam, Evaluation of cytotoxic and neuropharmacological activity of methanolic extract of solanum capsicoides leaves, Current Traditional Medicine 9 (2023), https://doi.org/10.2174/2215083809666221019150333.

[80] M.N.H. Zilani, T. Sultana, S.M. Asabur Rahman, M. Anisuzzman, M.A. Islam, J.A. Shilpi, M.G. Hossain, Chemical composition and pharmacological activities of Pisum sativum, BMC Compl. Alternative Med. 17 (2017) 171, https://doi.org/10.1186/s12906-017-1699-y.

[81] M.S. Kang, K.Y. Hyun, Antinociceptive and anti-inflammatory effects of Nypa fruticans wurmb by suppressing TRPV1 in the sciatic neuropathies, Nutrients 12 (2020), https://doi.org/10.3390/nu12010135.

[82] M.N.H. Zilani, M.A. Islam, P. Biswas, M. Anisuzzman, H. Hossain, J.A. Shilpi, M.N. Hasan, M.G. Hossain, Metabolite profiling, anti-inflammatory, analgesic potentials of edible herb Colocasia gigantea and molecular docking study against COX-II enzyme, J. Ethnopharmacol. 281 (2021) 114577, https://doi.org/10.1016/j.jep.2021.114577.

[83] K.K. Sarkar, T. Mitra, M.A. Rahman, I.M. Raja, M. Aktaruzzaman, M.A. Abid, M.N.H. Zilani, D.N. Roy, In vivo bioactivities of Hoya parasitica (wall.) and in silico study against cyclooxygenase enzymes, BioMed Res. Int. 2022 (2022), https://doi.org/10.1155/2022/1331758.

[84] M. Anisuzzman, M.M. Hasan, A.K. Acharzo, A.K. Das, S. Rahman, In vivo and in vitro evaluation of pharmacological potentials of secondary bioactive metabolites of dalbergia candenatensis leaves, Evid. base Compl. Alternative Med. 2017 (2017), https://doi.org/10.1155/2017/5034827.

[85] R.A. Moushome, M.I. Akter, M.A. Aziz, Phytochemical screening and antinociceptive and antidiarrheal activities of hydromethanol and petroleum benzene extract of microcos paniculata barks, BioMed Res. Int. 2016 (2016), https://doi.org/10.1155/2016/3167085.

[86] K. Nowotny, T. Jung, A. Höhn, D. Weber, T. Grune, Advanced glycation end products and oxidative stress in type 2 diabetes mellitus, Biomolecules 5 (2015) 194–222, https://doi.org/10.3390/biom5010194.

[87] N. Nahar, Md Nazmul Hasan Zilani, P. Biswas, Md Morsaline Billah, S. Bibi, N.A. Albekairi, A. Alshammari, Md Nazmul Hasan, Profiling of secondary metabolite and evaluation of anti-diabetic potency of Crotalaria quinquefolia (L): in-vitro, in-vivo, and in-silico approaches, Saudi Pharmaceut. J. 32 (2024) 101887, https://doi.org/10.1016/j.jsps.2023.101887.

[88] MdT. Islam, Md Aktaruzzaman, A. Saif, A. Akter, M.A. Bhat, M.M. Hossain, S.M.N. Alam, R. Rayhan, S. Rehman, M. Yaseen, MdO. Raihan, In silico-based identification of natural inhibitors from traditionally used medicinal plants that can inhibit dengue infection, Mol. Biotechnol. (2024), https://doi.org/10.1007/s12033-024-01204-8.

[89] N.H. Siddiquee, S. Malek, A.A. Tanni, I.J. Mitu, S.H. Arpa, M.R. Hasan, S.E.J. Shammi, C. Chakma, M. Mahinur, S. Wajed, M.I. Hossain, M. Aktaruzzaman, O. Saha, Unveiling the antiviral activity of 2′,3,5,7-Tetrahydroxyflavanone as potential inhibitor of chikungunya virus envelope glycoprotein, Inform. Med. Unlocked 47 (2024) 101486, https://doi.org/10.1016/j.imu.2024.101486.

[90] MdE.K. Talukder, Md Aktaruzzaman, N.H. Siddiquee, S. Islam, T.A. Wani, H.M. Alkahtani, S. Zargar, MdO. Raihan, MdM. Rahman, S. Pokhrel, F. Ahammad, Cheminformatics-based identification of phosphorylated RET tyrosine kinase inhibitors for human cancer, Front. Chem. 12 (2024), https://doi.org/10.3389/fchem.2024.1407331.